NASA TechBriefs

National Aeronautics and Space Administration

Electronic Components and Circuits

Electronic Systems

Physical Sciences

Materials

Computer Programs

Mechanics

Machinery

Fabrication Technology

Mathematics and Information Sciences

Life Sciences

98-12

December 1998

INTRODUCTION

Tech Briefs are short announcements of new technology derived from the research and development activities of the National Aeronautics and Space Administration. These Briefs emphasize information considered likely to be transferable across industrial, regional, or disciplinary lines and are issued to encourage commercial application.

Availability of NASA Tech Briefs and TSP's

Distribution of NASA Tech Briefs, a monthly periodical publication, is limited to engineers in U.S. Industry and to other domestic technology transfer agents. Requests for individual Tech Briefs or for Technical Support Packages (TSP's) announced herein should be addressed to

NASA Center for AeroSpace Information
Technology Transfer Office
800 Elkridge Landing Rd.
Linthicum Heights, MD 21090-2934
Telephone No. (301) 621-0245

Please reference the three-letter, five-digit control number located at the end of each Tech Brief. Information on NASA's Technology Utilization Program, its documents, and services is also available at the same facility.

Technology Utilization Officers and Patent Counsels are located at NASA field installations to provide technology-transfer access to industrial users. Inquiries can be made by writing to NASA field installations listed below.

Technology Utilization Officers and Patent Counsels

Ames Research Center
Technology Utilization Officer
Mail Code 223-3
Moffett Field, CA 94035

Patent Counsel
Mail Code 200-11
Moffett Field, CA 94035

Goddard Space Flight Center
Technology Utilization Officer
Mail Code 702-1
Greenbelt, MD 20771

Patent Counsel
Mail Code 204
Greenbelt, MD 20771

Lyndon B. Johnson Space Center
Technology Utilization Officer
Mail Code IC-4
Houston, TX 77058

Patent Counsel
Mail Code AL3
Houston, TX 77058

John F. Kennedy Space Center
Technology Utilization Officer
Mail Stop PT-PMO-A
Kennedy Space Center, FL 32899

Patent Counsel
Mail Code PT-PAT
Kennedy Space Center, FL 32899

Langley Research Center
Technology Utilization Officer
Mail Stop 143
Hampton, VA 23665

Patent Counsel
Mail Code 279
Hampton, VA 23665

Lewis Research Center
Technology Utilization Officer
Mail Stop 7-3
21000 Brookpark Road
Cleveland, OH 44135

Patent Counsel
Mail Code LE-LAW
21000 Brookpark Road
Cleveland, OH 44135

Jet Propulsion Laboratory
Technology Utilization Officer
Mail Stop 156-211
4800 Oak Grove Drive
Pasadena, CA 91109

NASA Resident Office-JPL
Technology Utilization Officer
Mail Stop 180-801
4800 Oak Grove Drive
Pasadena, CA 91109

Patent Counsel
Mail Code 180-801
4800 Oak Grove Drive
Pasadena, CA 91109

George C. Marshall Space Flight Center
Technology Utilization Officer
Code AT01
Marshall Space Flight Center, AL 35812

Patent Counsel
Mail Code CC01
Marshall Space Flight Center, AL 35812

John C. Stennis Space Center
Technology Utilization Officer
Code HA-30
Stennis Space Center, MS 39529

NASA Headquarters
Technology Utilization Officer
Code CU
Washington, DC 20546

Assistant General Counsel for Patent Matters
Code GP
Washington, DC 20546

Dryden Flight Research Center
Technology Utilization Officer
M/S D21-31
Bldg. 4832 Wheel 7
Lilly Dr.
Edwards, CA 93523

BLANK PAGE

NASA TechBriefs

December 1998
98-12

National Aeronautics and
Space Administration

BLANK PAGE

4

Electronic Components and Circuits

Hardware, Techniques, and Processes

BLANK PAGE

Ridged Tracks for Guiding Magnetic Bubbles

Ridges offer advantages over grooves.

NASA's Jet Propulsion Laboratory, Pasadena, California

Tracks for the guidance of magnetic bubbles propagating in the input and output lines of Vertical-Bloch-Line memory devices can be made in the form of ridges instead of in the traditional form of grooves. The ridge-type tracks offer advantages over the groove-type tracks, as explained below.

A track is formed on a substrate made of suitable magnetic material; namely, a garnet film. A gradient of the vertical magnetic field is associated with a step in the thickness of the film; the field increases as one proceeds from a location where the film is thinner to a location where it is thicker. Thus, in the case of a groove, the field increases as one crosses either wall of the groove from the inside to the outside. Because the stable position of a magnetic bubble lies at a local minimum of the field, a bubble that has been propagating along the groove remains confined in the groove.

The spatial variation of the field is, however, slightly more complex than is the spatial variation in thickness (see figure). The field increases slightly from the wall toward the middle of a groove. Thus, there are shallow local field minima along the sides of a groove. If the groove is wider than about 1.5 bubble diameters, then a bubble tends to move sometimes along one side, sometimes along the other side, moving back and forth in mostly random fashion as it propagates along the groove. If the groove is narrower than about 1.3 bubble diameters, a bubble remains centered in the groove but propagates more slowly than it would if the groove were wider. The customary groove width of 1.5 bubble diameters is a compromise that entails a little of both slowing down and meandering of bubbles.

A ridge-type track is formed by etching wide grooves on both sides of the track. Mirroring the situation in a groove, the magnetic field rises to maxima near the two side walls of the track, while at the middle of the track, the field falls to a local minimum that is isolated from the deeper minima of the adjacent grooves. The confinement gradient of a ridge is weaker than that of a groove, but still adequate for guidance. Unlike a groove track, a ridge track can be made wider than 1.3 bubble diameters without incurring meandering of bubbles; a ridge as wide as 2.5 bubble diameters can provide excellent guidance.

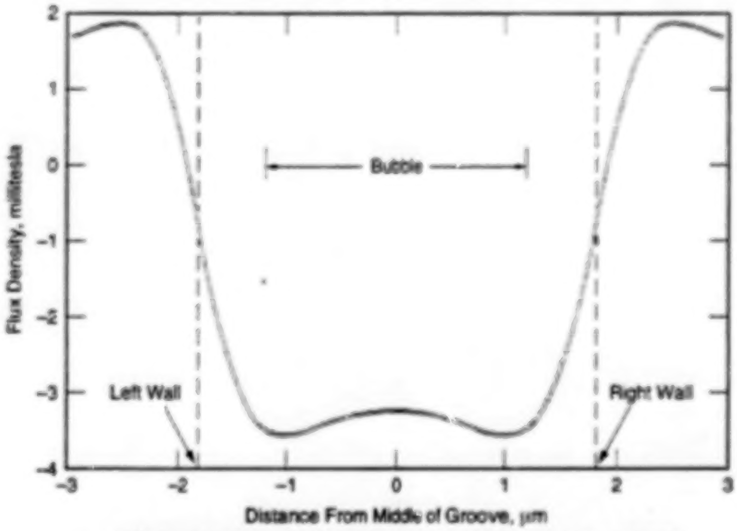

MAGNETIC FIELD OF A GROOVE 3.6 µm WIDE AND 0.5 µm DEEP (FOR CONFINING A MAGNETIC BUBBLE 2.4 µm WIDE)

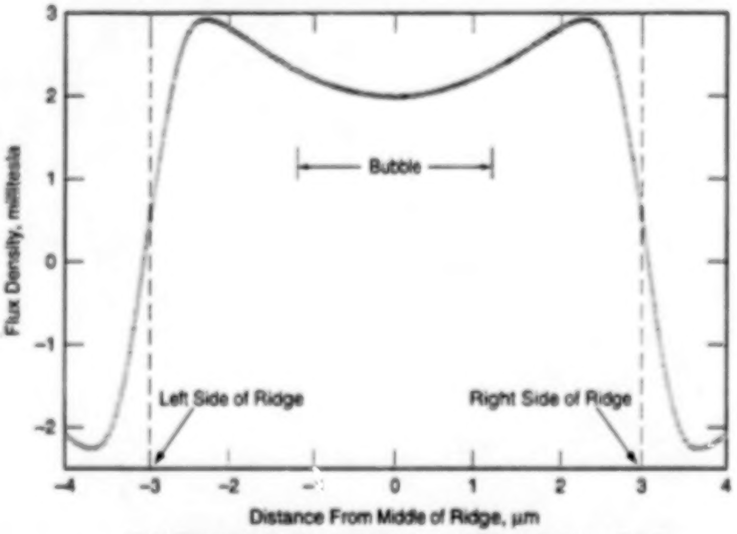

MAGNETIC FIELD OF A RIDGE 6.0 µm WIDE AND 0.5 µm DEEP (FOR CONFINING A MAGNETIC BUBBLE 2.4 µm WIDE)

The **Cross-Track Variation in the Permanent Magnetic Field** of the garnet film is what determines the magnetic-bubble-confining properties of the track.

Another advantage of a ridge-type track over a groove-type track arises in connection with the need to expand a bubble into a stripe when it reaches the end of the track, in preparation for detection of the bubble by use of a magnetoresistive strip. In the case of a groove-type track, the bubble expander is a mesa with its top recessed slightly below the surrounding garnet surface. An electric current in a helper loop is needed to provide a momentary additional magnetic field to lift a bubble from the groove, over the potential barrier at the edge of the mesa, so that the bubble can then stripe out on top of the mesa.

In the case of a ridge-type track, the track can simply be terminated in a mesa-type expander of the same height as that of the ridge. There being no step

discontinuity in height, there is no need for a helper loop to move the bubble out onto the expander.

This work was done by Udo Lieneweg of Caltech for **NASA's Jet Propulsion Laboratory**. *Further information is contained in a TSP [see page 1].*

In accordance with Public Law 96-517, the contractor has elected to retain title to this invention. Inquiries concerning rights for its commercial use should be addressed to

Technology Reporting Office
JPL
Mail Stop 122-116
4800 Oak Grove Drive
Pasadena, CA 91109
(818) 354-2240

Refer to NPO-20232, volume and number of this NASA Tech Briefs issue, and the page number.

Microlenses on Focal-Plane Arrays of QWIPs

Noise could be decreased or operating temperature increased.

NASA's Jet Propulsion Laboratory, Pasadena, California

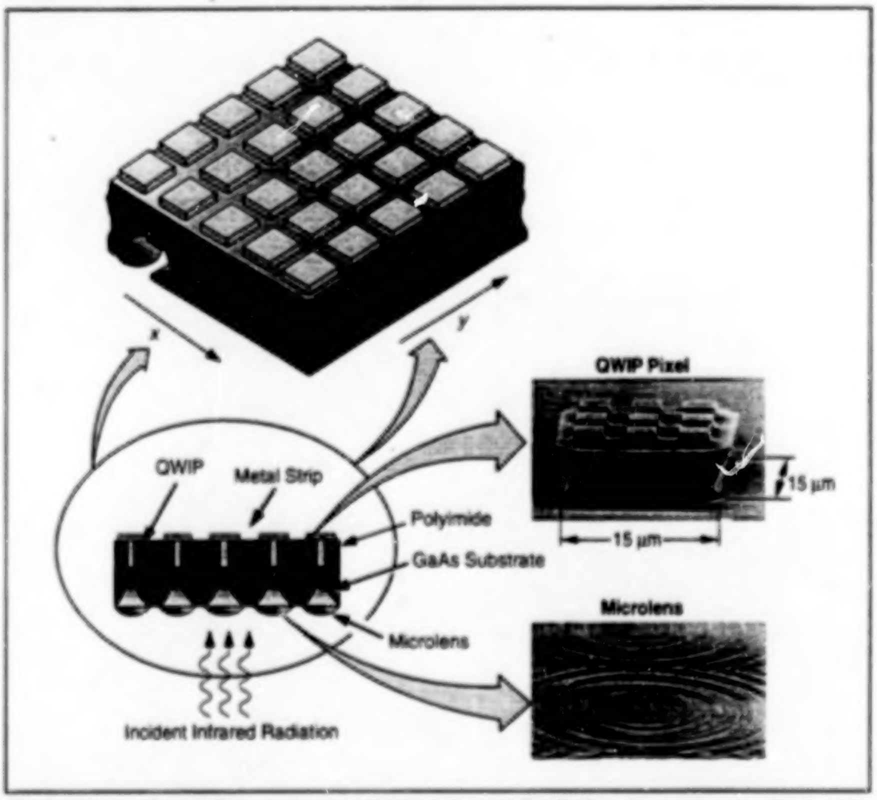

Microlenses Would Concentrate Incident Infrared Radiation (or preserve optical area) into areas smaller than those defined by the pixel pitch. The areas of the QWIPs could be reduced concomitantly to reduce dark current.

The performances of large focal-plane arrays of quantum-well infrared photodetectors (QWIPs) would be improved, according to a proposal, by incorporating microlenses. In comparison with a similar QWIP array that lacked microlenses, a QWIP array with microlenses could be made to exhibit less dark current [and thus a greater signal-to-noise ratio (SNR)] at a given temperature. Alternatively, the QWIP array with microlenses could be made to exhibit a given SNR at a higher temperature; this would be advantageous in that it would open up the possibility of operating QWIPs in infrared cameras at higher temperatures, reducing the cost of cooling the QWIPs to obtain adequate SNRs.

It would be advantageous to reduce dark current for two reasons:

1. The noise current of a photodetector is proportional to the square root of its dark current.
2. Along with signal current, dark current contributes to filling of the charge-storage wells of a readout multiplexer. Because of this and because the amount of charge that can be stored is finite, the available charge-integration time decreases with increasing dark current. As the charge-integration time decreases, the SNR decreases.

Assuming that the QWIPs in a given array were designed to operate with back-side illumination, the microlenses would be formed on the back side (the substrate side) of the array (see figure). There would be one microlens for each pixel. The basic function of the microlenses would be to concentrate incident infrared radiation (or preserve optical area) into a fraction of the area of each pixel. Concomitantly, the active device area in each pixel would be reduced to encompass only the reduced illuminated area plus (if desired) an appropriate margin. Inasmuch as the dark current of a QWIP is proportional to its area, the dark current would be reduced accordingly.

Suppose, for example, that a QWIP array had a 50-μm pixel pitch with active pixel areas of 45 by 45 μm. Microlenses could be used to concentrate light into 15-by-15-μm active pixel areas. If the active pixel areas were reduced to 15 by 15 μm, then the dark current at a given temperature would be reduced to 1/9 of its previous value, and therefore, the noise current at that temperature would be reduced to 1/3 of its previous value.

This work was done by Sarath Gunapala, Sumith Bandara, and Fred Pool of Caltech for **NASA's Jet Propulsion Laboratory**. *Further information is contained in a TSP [see page 1].*

In accordance with Public Law 96-517, the contractor has elected to retain title to this invention. Inquiries concerning rights for its commercial use should be addressed to

Technology Reporting Office
JPL
Mail Stop 122-116
4800 Oak Grove Drive
Pasadena, CA 91109
(818) 354-2240

Refer to NPO-20309, volume and number of this NASA Tech Briefs issue, and the page number.

Trenches Would Reduce Cross-Talk Among Microlensed QWIPs

Less scattered light would impinge on neighboring pixels.

NASA's Jet Propulsion Laboratory, Pasadena, California

Cross-talk in integrated-circuit focal-plane arrays of quantum-well photodetectors (QWIPs) equipped with microlenses would be reduced, according to a proposal, by etching deep trenches into the substrates of these devices. The proposal applies, more specifically, to GaAs-based, back-side-illuminated QWIP arrays with microlenses — devices like those described in the preceding article.

The cross-talk problem in such a device without trenches would arise as follows: The microlenses would be formed by patterning the back side of the substrate, as described in the preceding article. The lenses would focus the incident infrared light into and through subpixel-size active device (QWIP) areas. Most of the focused light would not be absorbed by the QWIPs, due to lower quantum efficiency, and would, instead, be scattered from patterned reflective surfaces on the front side. A significant portion of the light scattered in each pixel would travel through the unthinned substrate to neighboring pixels, where some of it would be absorbed, thereby giving rise to cross-talk. The cross-talk-reduction problem would thus become one of preventing the scattered infrared light from traveling through the substrate to neighboring pixels.

The problem could not be solved by thinning the entire substrate to the membrane level because such thinning would make it impossible to achieve the required focal length of the microlenses. The proposal would afford the optical advantage of microlenses, without the optical disadvantage of thinning the entire substrate. Instead of thinning the entire substrate, one would etch the substrate only along the boundaries between neighboring pixels; in other words, one would etch deep trenches in the substrate between microlens/pixel units. Such trenches are shown in the figure of the preceding article. Because of the large difference between the indices of refraction of air and the GaAs substrate, the trenches would be highly effective as optically isolating cavities to reduce cross-talk.

This work was done by Sarath Gunapala, Sumith Bandara, and John Liu of Caltech for **NASA's Jet Propulsion Laboratory**. *Further information is contained in a TSP [see page 1].*

In accordance with Public Law 96-517, the contractor has elected to retain title to this invention. Inquiries concerning rights for its commercial use should be addressed to

Technology Reporting Office
JPL
Mail Stop 122-116
4800 Oak Grove Drive
Pasadena, CA 91109
(818) 354-2240

Refer to NPO-20311, volume and number of this NASA Tech Briefs *issue, and the page number.*

Bound-to-Quasi-Bound QWIPs With Random Reflectors

Dark currents are reduced and light-coupling efficiencies increased.

NASA's Jet Propulsion Laboratory, Pasadena, California

Quantum-well infrared photodetectors (QWIPs) that are designed to exploit transitions between bound and quasi-bound electron quantum states and that incorporate random reflectors are undergoing development. Focal-plane arrays of such detectors are also undergoing development, all as part of a continuing effort to increase the responsivities and decrease the noise levels (dark currents) of infrared-imaging devices operating at wavelengths from about 3 to about 18 µm.

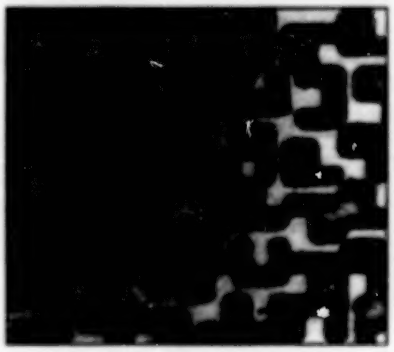

RANDOM REFLECTOR ON ONE PIXEL OF A 128-by-128 ARRAY WITH A CUTOFF WAVELENGTH OF 15 µm

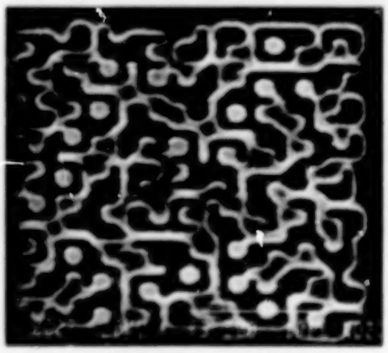

RANDOM REFLECTOR ON ONE PIXEL OF A 256-by-256 ARRAY WITH A CUTOFF WAVELENGTH OF 9 µm

Each of These Random Reflectors was fabricated on one pixel of a focal-plane array of QWIPs. In the one on the left, the minimum feature size is 1.25 µm; in the one on the right, the minimum feature size is 0.6 µm.

QWIPs have been discussed in numerous prior articles in *NASA Tech Briefs*. Two articles with particular relevance to the present devices were "Bound-to-Quasi-Bound Quantum-Well Infrared Photodetectors" (NPO-19633), Vol. 22, No. 9 (September 1998), page 54 and "Demonstration of 15 µm 128 × 128 Quantum Well IR Photodetector Imaging Camera" (NPO-19407) Vol. 20, No. 11 (November 1996), page 30. The first-mentioned article discussed, in some detail, the advantage of designing QWIPs to exploit bound-to-quasi-bound transitions to reduce dark currents below those achievable in QWIPs that exploit bound-to-continuum transitions. The second-mentioned article included a passing mention of the use of random reflectors to increase the efficiency of coupling of light into the QWIPs. In the time since the second-mentioned article, more information on the random reflectors has become available, and is presented below.

The light-coupling problem was discussed in yet another prior article; namely,

"Cross-Grating Coupling for Focal-Plane Arrays of QWIPs" (NPO-19657), *NASA Tech Briefs*, Vol. 22, No. 1 (January 1998), page 6a. To recapitulate: (1) The direction through the thicknesses of the quantum wells is parallel to the focal plane; (2) Quantum selection rules allow the detection of only that part of the incident light that is electrically polarized along the direction through the thicknesses of the quantum wells and thus perpendicular to the focal plane; and (3) The light to be detected is incident along directions approximately perpendicular to the focal plane, and thus only a small fraction of it is electrically polarized along the thicknesses of the quantum wells. Prior to the development of the random reflectors, light-coupling efficiency was increased by illuminating QWIPs via facets inclined 45° to the directions through the thicknesses of their quantum wells. However, the 45° coupling scheme is not suitable for two-dimensional imaging arrays of QWIPs. The random-reflector scheme is suitable for two-dimensional arrays.

Many more passes of infrared light inside a QWIP, with a corresponding increase in responsivity over that achievable with a 45° facet, can be obtained by incorporating a randomly roughened reflecting surface on top of the QWIP. The random structure of the reflector prevents the light from being diffracted perpendicularly backward after the second bounce, as happens in the case of a cross-grating coupling like that discussed in the third-mentioned prior article. After each bounce, light is scattered at a different random angle, and the only chance for light to escape from the detector occurs when it is reflected toward the surface within the critical angle of the perpendicular. For a GaAs/air interface, this angle is about 17°, defining a very narrow escape cone for the trapped light.

The QWIP in each pixel of an array according to the present design concept contains a random reflector (see figure) with scattering surfaces at two levels separated by a quarter of the wavelength of interest in GaAs. The area of the top (unetched) level equals the area of the bottom (etched) level. The combination of equal areas and quarter-wavelength separation maximizes the destructive interference of light reflected from the two levels along the perpendicular, thus limiting the leakage of light through the escape cone.

This random reflector structure can be fabricated by use of standard photolithography and selective dry etching with CCl_2F_2. The advantage of photolithography over a completely random fabrication process is the ability to accurately control the sizes of features to preserve pixel-to-pixel uniformity.

This work was done by Sarath Gunapala, John K. Liu, Mani Sundaram, and Jin S. Park of Caltech for **NASA's Jet Propulsion Laboratory**. *Further information is contained in a TSP [see page 1].*

In accordance with Public Law 96-517, the contractor has elected to retain title to this invention. Inquiries concerning rights for its commercial use should be addressed to

Technology Reporting Office
JPL
Mail Stop 122-116
4800 Oak Grove Drive
Pasadena, CA 91109
(818) 354-2240

Refer to NPO-19815, volume and number of this NASA Tech Briefs *issue, and the page number.*

Electronic Systems

Hardware, Techniques, and Processes

BLANK PAGE

Update on the Web Interface for Telescience

The interface software is automatically downloaded by use of web-browser software.

NASA's Jet Propulsion Laboratory, Pasadena, California

An Internet-based software system called the "Web Interface for Telescience" (WITS), enables geographically dispersed scientists to participate in scientific exploration of remote planets by use of instrumented landers and robotic vehicles called "rovers." WITS at a previous stage of development was described in "Web Interface for Telescience" (NPO-19934), *NASA Tech Briefs*, Vol. 21, No. 8 (August 1997), page 34. Since that description was published, major additional features have been incorporated. Originally intended for use in a rover mission on Mars in the year 2001, WITS reached sufficient maturity early enough to have limited use during the 1997 Mars *Pathfinder* mission. Also, WITS will be used in the 1998 Mars Polar Lander mission.

One basic purpose of WITS is to enable mission scientists at their home institutions to collaborate, quickly and efficiently, in planning planetary robot operations without having to travel to a central control station at NASA's Jet Propulsion Laboratory. This is accomplished by use of interactive displays of images of terrain from rover-mounted video cameras, terrain maps derived from such images, and other data from rover-mounted instruments. Provisions for measuring and annotating terrain features and planning mission activities are included in the displays. Scientists and engineers can, for example, use WITS displays to enter such command data as way points on a traversal of terrain, plus scientific observations and/or engineering tasks that the rover must perform at some or all way points.

Another basic purpose served by WITS is to communicate mission data to the public as quickly as possible. To serve this purpose while providing an element of security, WITS is constructed as two physically separate, parallel systems: the mission system and the public system (see figure). Both systems receive data updates from the rover mission, and both systems contain the same software, including software for planning rover tasks. However, only the mission system commands the rover. The planning software in the public system can be used only to perform simulations that reside solely on users' computers. In other words, the mission and public systems are nearly identical, except that data are not transmitted from the public to the mission system.

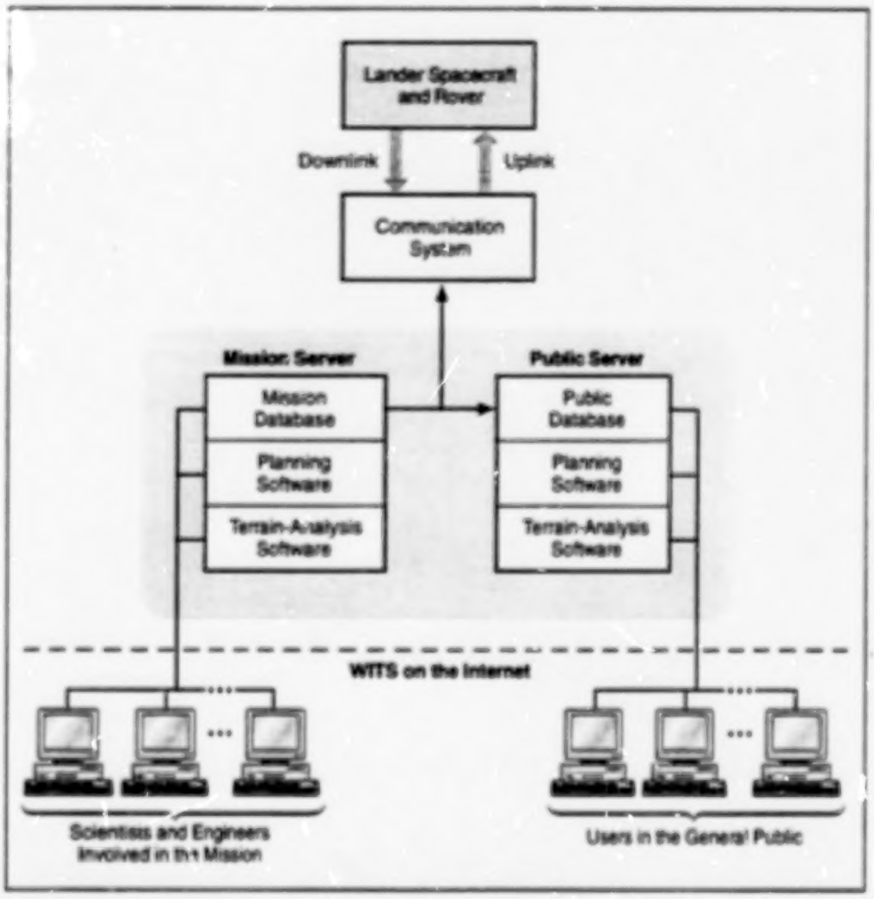

Geographically Dispersed Computer Users have access to rover-mission data, though only scientists and engineers directly involved in the mission can affect the mission. Members of the general public can use planning software to plan and simulate rover activities on their local computers only.

The WITS software is divided into two parts: (1) the client part, which is executed on a user's computer, and (2) the server part, which is executed on one server computer for the mission system and on another server computer for the public system. The servers communicate with the clients and perform such computationally intensive operations as processing of stereoscopic images and generation of range maps. The mission server also acts as an interface with the communication system that conveys data to and from the rover and its spacecraft. The servers maintain a common data base, including information on the current mission plan. Collaboration is greatly facilitated in that the same video images, instrument readouts, and planning information can be viewed simultaneously by all users. However only mission participants (who must prove authorization by logging onto the mission server by use of passwords) can modify the common data base.

The client part of the WITS software is written in the Java computing language as a Java applet and is automatically downloaded onto the user's computer by the user's own web-browser software. This feature makes WITS available to many users and executable on almost any computer at any site. The great advantages of this feature are that the collaborating team and public audience can be expanded at little cost, and that each user has immediate access to the most recent version of the client part of the WITS software.

This work was done by Paul Backes of Caltech and Kam S. Tso and Greg Tharp of IA Tech, Inc., for **NASA's Jet Propulsion Laboratory**. *Further information is contained in a TSP (see page 1).*
NPO-20374

Program for Analyzing Free-Space Optical Communication Links

This easy-to-use program does not require detailed knowledge of optical components.

NASA's Jet Propulsion Laboratory, Pasadena, California

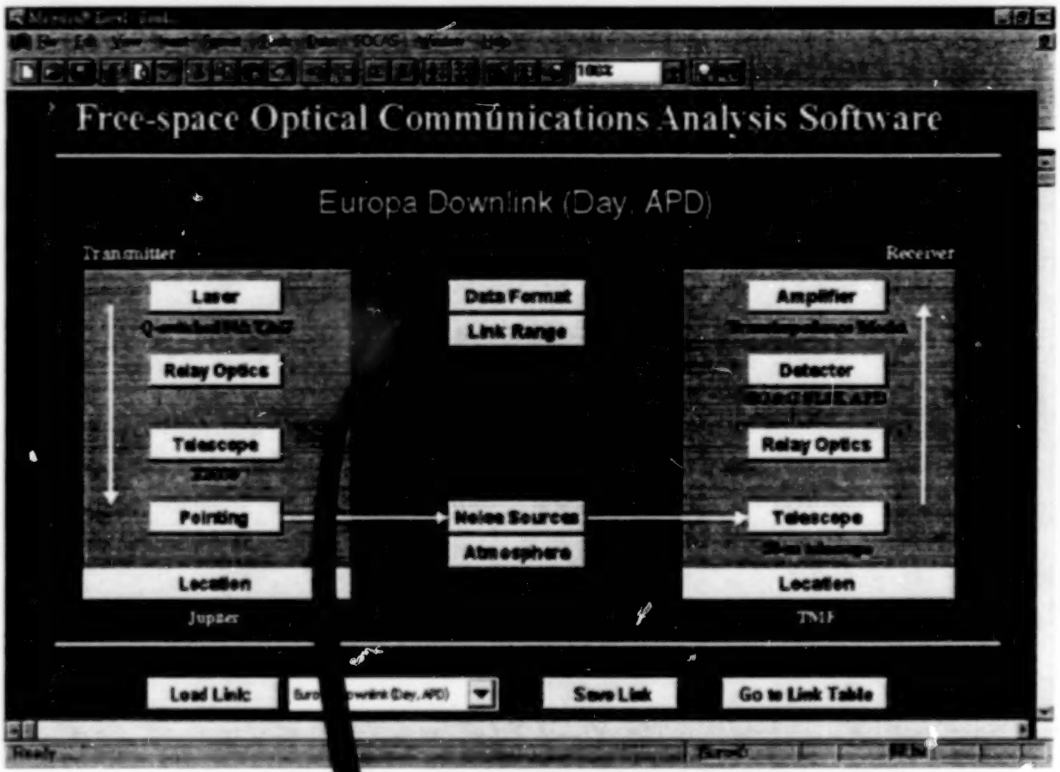

DISPLAY CONTAINING A BLOCK DIAGRAM

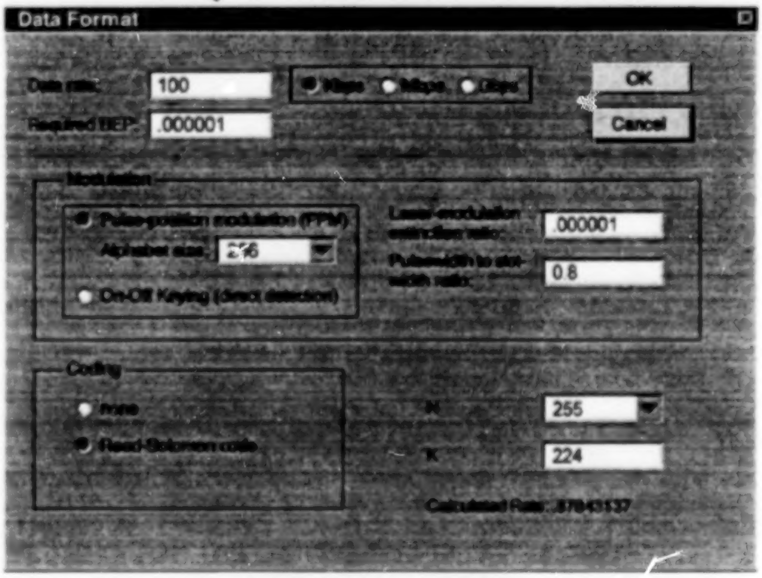

EXAMPLE OF A DIALOG BOX

FOCAS Displays a Block Diagram of an optical communication link. Through each block in the diagram, the user can bring up a dialog box (in this example, the Data Format box) to edit parameters of the aspect of the link represented by the block.

"Free-Space Optical Communications Analysis Software" (FOCAS) is the name of a spreadsheet computer program for analysis of direct-detection (as distinguished from heterodyne-detection) optical data-communication links. Implemented within the Microsoft Excel software system, FOCAS exploits the flexibility and power of the Excel spreadsheet features. An easy-to-use graphical user interface to the spreadsheet has been developed in Visual Basic for Applications to facilitate insertion of parameters of optical components and of other input data. Optionally, the user can select the automatic insertion of parame-

ters from a data base of known commercial components. Thus, even nonexperts who lack detailed knowledge of optical components can perform analyses.

The following is a partial list of communication-link features accommodated in FOCAS.

- Modulation schemes: on/off keying and M-ary pulse-position modulation, including Manchester coding (binary PPM) as a special case of M-ary PPM.
- Coding: Reed-Solomon code with choice of code-word length and number of information symbols.
- Lasers: Energy-storage-based pulsed lasers or continuous-wave lasers with current modulation or external modulators.
- Transmitter and Receiver Optics: Gains, beam widths, and related parameters are calculated for Gaussian or near-diffraction-limited beam profiles. The effect of transmitting-telescope wavefront quality is incorporated in the Strehl ratio.
- Detectors: Quantum efficiencies of positive/intrinsic/negative (PIN) photodetectors, avalanche photodetectors (APDs) and photomultiplier tubes (PMTs) are represented by lookup tables. Gaussian statistics are used for PIN photodetectors and APDs; Poisson statistics are used for PMTs.
- Amplifiers: Noise, frequency response, and other characteristics of transimpedance and high-impedance preamplifiers can be obtained by use of mathematical models or by selection of amplifiers listed in the data base.
- Other: Wavelength- and zenith-angle-dependent atmospheric-transmission data and wavelength-dependent sky-radiance data are obtained from another program called "MODTRAN." By use of a Rician probability model, FOCAS calculates burst error probability due to pointing jitter and bias. Link ranges are determined automatically for given transmitter and receiver locations.

When FOCAS is opened in Excel, the program displays a block diagram of an optical communication link, including a transmitter, a free-space optical communication medium or channel containing noise sources, and a receiver (see figure). Each block in the diagram appears as a button that can be pressed to bring up a dialog box, through which the user can view and edit the parameters of the transmitting or receiving component, transmitting or receiving subsystem, channel, or link characteristic represented by the block. Other buttons below the block diagram enable the user to load or save parameters or view a link table, which is described below.

In a typical case, the user clicks on the buttons to enter the link parameters manually or, where desired, automatically by selection of a component from the data base. FOCAS automatically compares each parameter with minimum and maximum values to generate a warning and/or prevent the entry of a physically unrealistic value; for example, if the user attempts to enter a beam width less than the diffraction-limit minimum for a selected telescope diameter, then FOCAS displays an error message and does not allow the user to proceed further until the user enters a larger, realistic value.

Once all input parameters have been entered, the user can cause the program to display the link table by pressing the "Go to Link Table" button. The link table is a spreadsheet that shows both the input parameters and the values calculated by the program. The link table is divided into a link summary and a detailed link section. The link summary section contains parameters that characterize the overall link, including the overall link margin, link range, data rate, bit-error rate, transmitted power, received power, power required to achieve a specified overall link margin, transmitter gain, receiver gain, and terms that account for losses along the link path. The detailed link section follows the link summary section and consists of subsections (transmitter, channel, receiver, link margin, coding, calculation of required signal power, and background radiation), each of which provides information in depth on one aspect of the link.

Almost all of the cells in the link table are locked to prevent the user from inadvertently changing dependent variables calculated by the program. However, the user would find it inconvenient to go back to the dialog boxes to change the values of some common parameters in performing a series of related analyses. Therefore, FOCAS allows some of the parameters (for example, the link range, data rate, average laser power, width of the transmitted beam, and the diameter of the receiver aperture) to be changed in the link table. Following such changes, the auto-calculation feature of Excel updates the remainder of the link table; thus, FOCAS provides an interactive means of designing an optical communication link.

This work was done by Muthu Jeganathan, G. Stephen Mecherle, and James Lesh of Caltech for **NASA's Jet Propulsion Laboratory**. *Further information is contained in a TSP [see page 1].*
NPO-20412

Eight-Channel WDM Fiber-Optic Data-Communication System

Each channel would carry data at a rate up to 2.5 Gb/s.

John F. Kennedy Space Center, Florida

A proposed wavelength-division-multiplexing (WDM) optical communication system would feature a single optical fiber carrying eight channels of digital data signals. In the original application, the signal in each channel would be a serial digital video-camera output, but the system could just as well be used to convey other serial data streams. The data rate in each channel could be as high as 2.5 Gb/s.

The center wavelengths in the eight channels would range from 1,535.04 to 1,557.37 nm, and are chosen to obtain an interval of 400 GHz between the center frequencies of adjacent channels. The transmitter for each channel would be a distributed-feedback laser with a modulation frequency band of 50 kHz to 2.5 GHz. Each transmitter would accept input data signals at the emitter-coupled-logic (ECL) level. Because the laser transmitters would be subject to thermal wavelength drift, a feedback-controlled thermoelectric cooler would be used to maintain constant temperature and thereby prevent the middle frequency of the laser of each channel from drifting into the adjacent channel. The channel separation of 400 GHz would provide a margin against any drift due to a harsh environment, such as the space shuttle launch pads.

The optical fiber would be of the single-mode type. The outputs of the transmitters would be wavelength-multiplexed and coupled into the optical fiber by one of several alternative devices: a simple power coupler, a diffraction-grating-based coupler, an arrayed waveguide grating, or an interference-filter-based coupler. In choosing one

of these devices for a specific application, one would have to consider the following characteristics, among others: A diffraction-grating-based coupler would offer minimum insertion loss for each channel, but would be less thermally stable than an interference-filter-based coupler would be. On the other hand, in an interference-filter-based coupler, the insertion loss in each successive channel would be additive.

At the receiving end of the optical fiber, the signals would be wavelength-demultiplexed. With the exception of the simple power coupler, any of the three wavelength-multiplexing devices mentioned above could be used as the demultiplexer. The wavelength-demultiplexed optical signals would be fed to separate receivers for conversion to electrical data signals. The receivers would be capable of detecting infrared radiation at wavelengths from 1,200 to 1,600 nm. The electrical outputs of the receivers would be at the ECL level.

This work was done by William T. Toler of **Kennedy Space Center** *and Robert W. Swindle and F. Houston Galloway of formerly of I-NET. Further information is contained in a TSP [see page 1].*

Inquiries concerning rights for the commercial use of this invention should be addressed to the Technology Programs and Commercialization Office, Kennedy Space Center, (407) 867-6373. Refer to KSC-11974.

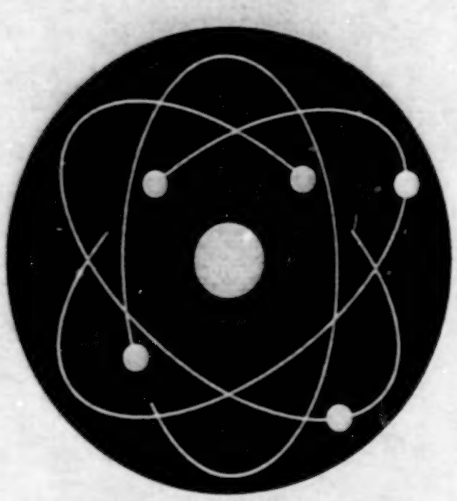

Physical Sciences

Hardware, Techniques, and Processes

BLANK PAGE

Evaluation of Exhaust Flows From Thrust-Vectoring Nozzles

A unique dual-flow cold-jet facility supports flight research programs.

Dryden Flight Research Center, Edwards, California

A unique dual-flow, cold-jet facility has been developed and operated by California Polytechnic State University (Cal Poly) at San Luis Obispo for NASA Dryden Flight Research Center. The facility supports flight research on thrust-vectoring nozzles and thrust-vector control systems. To date, the facility has completed tests on subscale nozzles of the F/A-18 *H*igh *A*lpha *R*esearch *V*ehicle (HARV), the X-31 airplane, and the F-15 *A*dvanced *C*ontrol *T*echnology for *I*ntegrated *V*ehicl*e*s (ACTIVE).

The facility contains a nozzle flow bench (see Figure 1) that incorporates unique features for research on single nozzles and on twin nozzles, which afford the ability to evaluate flow-interaction phenomena. Subscale nozzles are typically mounted on top of a thrust stand on the bench and connected to the end of an airflow-supply tube. The thrust stand is of a multiaxis design that affords capabilities for measuring all components of thrust and moment vectors.

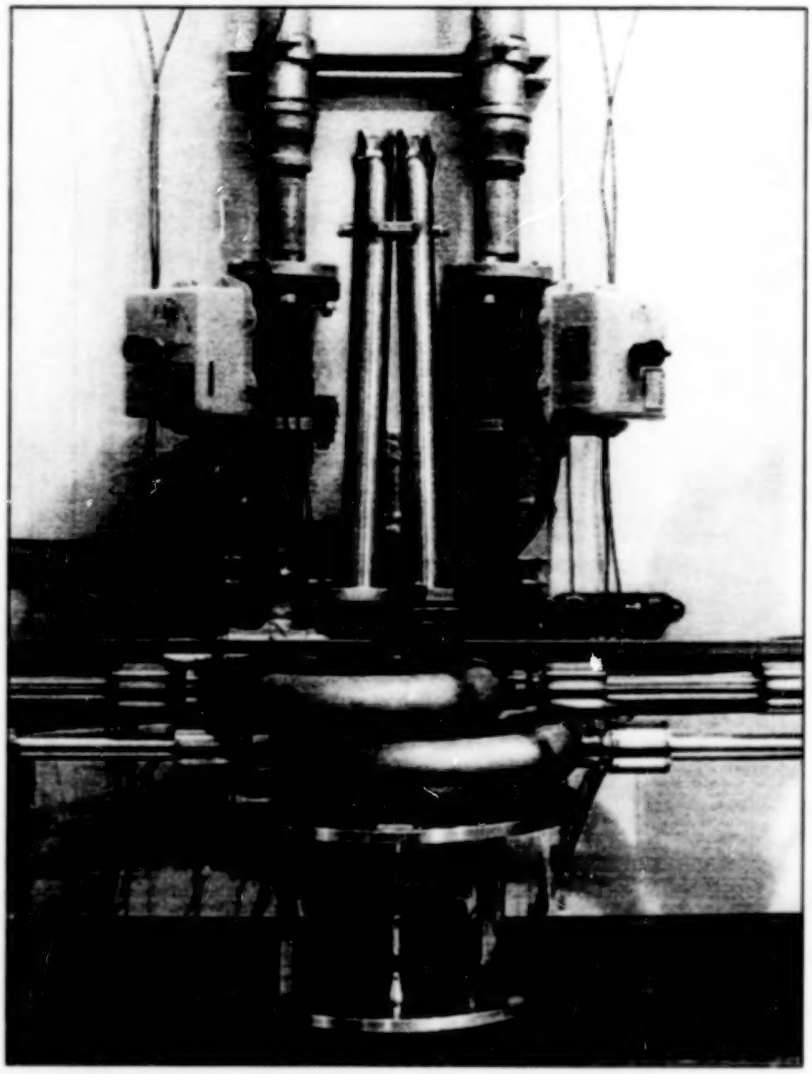

Figure 1. The **Equipment on the Nozzle Flow Bench** typically includes subscale nozzles mounted on top of a thrust stand and connected to a source of pressurized air via a manifold system that suppresses spurious air-supply-related side loads. The thrust stand enables measurement of all components of thrust and moment vectors.

A manifold system that supplies air to each nozzle independently is designed to avoid the introduction of extraneous side loads. The manifold system includes a plenum and bellows. Airflows at approximately equal rates are supplied on opposite sides of the plenum in order to cancel momentum and pressure effects that could otherwise be attributed to the air supply. This manifold design virtually eliminates extraneous forces from the air supply. In the dual-flow configuration, the flow rate or pressure ratio of each nozzle is independently controlled, providing maximum flexibility in testing.

The development of both the thrust stand and the air-supply manifold has made it possible to perform accurate research on thrust vectoring with small-scale nozzles. A capability for color schlieren photography has also been developed, making it possible to obtain visible records of complicated exhaust-flow fields and shock structures (for example, see Figure 2). A color schlieren video apparatus has also been built for use in evaluating the stability of exhaust -flow fields.

To verify the accuracy of the cold jet, a single 1/24-scale F/A-18 HARV nozzle configured with postexit vanes was tested in this facility, and the results of the tests were compared with those of similar tests performed on a larger-scale model at Langley Research Center. These tests also enabled detailed evaluation of a postexit-vane-tip interference effect that was pronounced at higher pressure ratios.

Additional single-nozzle tests were performed on the X-31 nozzle configuration to evaluate the effects of extreme deflections of postexit vanes. Static-pressure ports were added to the divergent section of the nozzle to obtain data pertinent to concerns about operability. The results of these tests supported the implementation of a 10° increase in deflections of nozzle postexit vanes on the X-31 airplane during its flight-test program, helping the aircraft achieve greater maneuverability.

One of the two-nozzle configurations shown Figure 2 was tested to explore the effects of flow interaction during thrust vectoring of the F/A-18 HARV. One of the main objectives of the tests was to validate a superposition assumption used in the design of the F/A-18 HARV thrust-vector control law. The assumption in question is that exhaust plumes from the two nozzles do not interact with each other and thus their total-force vector can be determined by

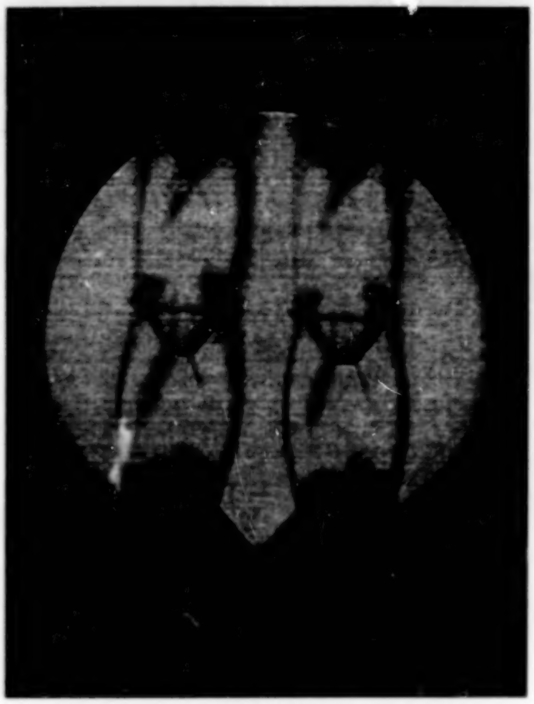

Two Nozzles in F/A-18 HARV Configuration

Two-Dimensional Nozzle (TheTransparent One) and Three Dimensional Axisymmetric Nozzle Side by Side

Photos courtesy of Cal Poly.

Figure 2. These **Schlieren Photographs** reveal some aspects of the exhaust flows from scale-model pairs of thrust-vector nozzles in cold-jet tests.

summing the force vectors of the individual nozzles as modeled in single-nozzle cold-jet tests. The aforementioned tests were the first documented tests to validate this superposition assumption. The results of the tests were found to support this superposition assumption, except at extreme vector angles, where one nozzle could impinge on a postexit vane of the other nozzle.

At present, the facility is testing thrust-vectoring nozzles with axisymmetric configurations, similar (except in scale) to full-scale, productionlike axisymmetric thrust-vectoring nozzles that are undergoing flight testing on the F-15 ACTIVE aircraft. The sub-scale-nozzle tests in the facility support the F-15 ACTIVE flight-test program. The results of in-flight measurements of nozzle vector plume angles have been found to differ significantly from those of corresponding measurements in subscale tests. The source of these differences has not yet been discovered, but finding this source is the primary goal of both the cold-jet (subscale) and the flight tests.

More specifically, 1/32-scale fixed-geometry vectored nozzles are undergoing tests in the facility. The primary immediate objectives of the cold-jet tests are to (1) attempt to reproduce the flight-measured vector plume angles and (2) evaluate and determine the locations and number of internal nozzle pressure sensors needed to measure in-flight pressure distributions accurately.

In addition, the tests accommodate some basic research on flow separation and stability. A unique test of a transparent two-dimensional nozzle has provided insight into the internal flow field of an axisymmetric thrust-vectoring nozzle. Part of Figure 2 presents images of the two-dimensional nozzle and a three-dimensional axisymmetric nozzle undergoing a test side by side at equal pressure ratios, vector angles, and throat and exit-area conditions. These tests have shown that the shocks inside the nozzles exert significant influence on the exhaust-flow field during thrust vectoring. Additional tests on axisymmetric nozzles instrumented with internal static-pressure probes are under way.

The data obtained in the facility have provided significant support to NASA's research on thrust-vectoring nozzles. Its relatively small scale and innovative approach have resulted in accurate, relatively inexpensive, and rapid testing, with such unique capabilities as its dual-flow capability. The schlieren photographic capability provides a valuable insight into flow-field properties, and the schlieren photographs augment the force and moment data traditionally available from cold-jet facilities.

This work was done by Albion H. Bowers, John S. Orme, and Ronald J. Ray of **Dryden Flight Research Center** *and Thomas Carpenter and Jim Gerhardt of California Polytechnic State University. Further information is contained in a TSP [see page 1].*

In accordance with Public Law 96-517, the contractor has elected to retain title to this invention. Inquiries concerning rights for its commercial use should be addressed to

Thomas Carpenter
California Polytechnic State University, San Luis Obispo
Department of Mechanical Engineering
San Luis Obispo, CA 93407
(805)756-1303

Refer to DRC-97-49, volume and number of this NASA Tech Briefs issue, and the page number.

Miniature, Tunable, Wide-Band-Pass Optical Filters

Short-cavity Fabry-Perot filters would offer wide tuning ranges.

NASA's Jet Propulsion Laboratory, Pasadena, California

A proposed miniature, electrically tunable, band-pass optical filter would have a Fabry-Perot configuration, but would be designed to trade the high spectral resolution (narrow-band pass) and small tuning range of a traditional Fabry-Perot filter for low spectral resolution (wide-band pass) and a wide tuning range. Filters like this are candidates to supplant two other types of optical filters used in remote-sensing spectrometers; namely, acousto-optical tunable filters (which are heavy and power hungry) and liquid-crystal tunable filters (which exhibit low efficiency and work only in narrow temperature ranges).

A Fabry-Perot filter can be characterized as an interference filter and as a resonant optical cavity. It comprises a cavity bounded by partially reflective, low-absorption mirror coats on two flat, transparent plates. A traditional Fabry-Perot filter is a high-spectral-resolution (narrow-band-pass), narrow-tuning-range device constructed with low-absorption mirror coats and a cavity that is many wavelengths long. In the proposed filters, the traditional low-absorption mirror coats would be replaced by lossy metal coats only a few tens of nanometers thick, making the optical properties partly dependent on the choice of metal. In addition, the cavities would be shortened to less than one wavelength, increasing the tuning ranges for given small displacements; for example, as described below, if the distance between lossy mirror coats were made variable from 150 to 300 nm, then the tuning range would span the spectrum of visible light.

A typical proposed filter (see Figure 1) would include two glass plates with silver mirror coats 40 nm thick, separated by an airgap about half a wavelength thick. The gap thickness (cavity length) would be established by piezoelectric spacers. Thus, the filter could be tuned by applying a suitable voltage to the spacers. Figure 2 shows the calculated transmission spectra for various cavity lengths; the wavelength of peak transmission would range from 410 nm at a cavity length of 150 nm to 700 nm at a cavity length of 300 nm.

In another example, the mirror coats would be made of potassium 100 nm thick, making it possible to obtain an infrared pass band. The calculated transmission spectra for this example are also shown in Figure 2. In this case, the wavelength of peak transmission would range from 800 nm at a cavity length of 300 nm to 1,400 nm at a cavity length of 600 nm.

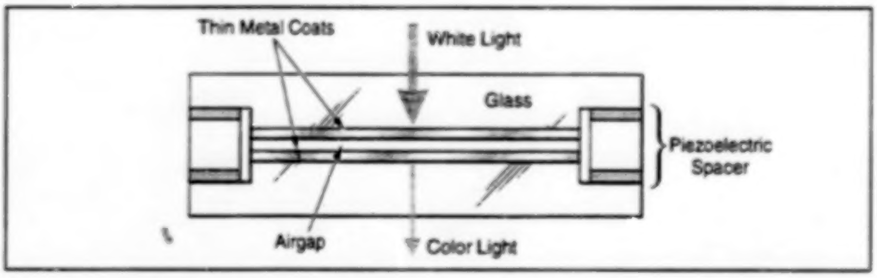

Figure 1. A **Short-Cavity Fabry-Perot Filter** would be tuned by adjusting the voltage applied to piezoelectric spacers.

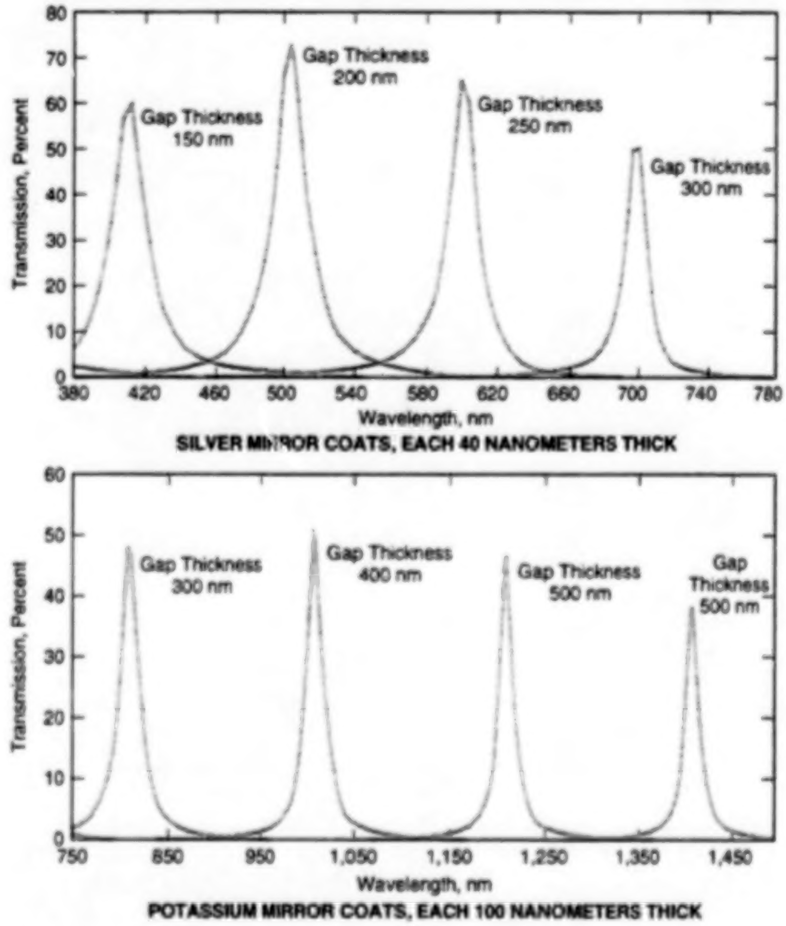

Figure 2. The **Peak of the Transmission Spectrum Would Shift** with a change in the gap thickness.

This work was done by Yu Wang of Caltech for **NASA's Jet Propulsion Laboratory**. *Further information is contained in a TSP [see page 1].*

In accordance with Public Law 96-517, the contractor has elected to retain title to this invention. Inquiries concerning rights for its commercial use should be addressed to

Technology Reporting Office
JPL
Mail Stop 122-116
4800 Oak Grove Drive
Pasadena, CA 91109
(818) 354-2240

Refer to NPO-20245, volume and number of this NASA Tech Briefs issue, and the page number.

Monolithic Electrostatic Sector for Miniature Mass Spectrometers

The cost of fabrication is reduced considerably.

NASA's Jet Propulsion Laboratory, Pasadena, California

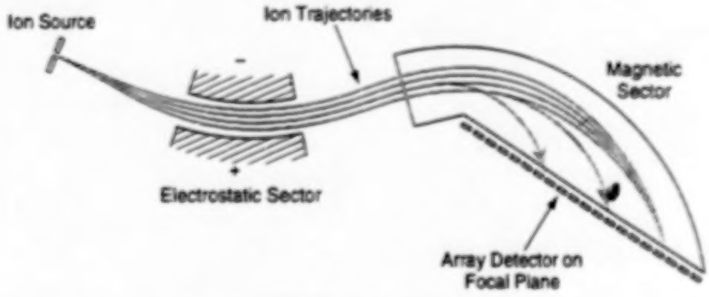

SIMPLIFIED PLAN VIEW

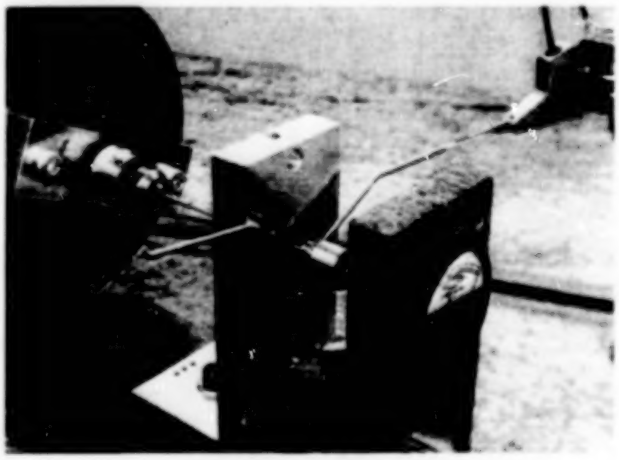

PHOTOGRAPH OF PROTOTYPE

A **Mass Spectrometer of Mattauch-Herzog Geometry** includes an electrostatic sector plus a magnetic sector that ends in an array detector on a focal plane. The electrostatic sector is made from a single piece of machinable ceramic and has a mass of only 30 g.

An improved miniature electrostatic sector has been designed for a miniature double-focusing mass spectrometer (see figure). Miniature mass spectrometers are essential components of high-performance, miniature, low-power instruments that are being developed for use in analyzing chemical compositions of small amounts of substances (e.g., toxic chemicals in the environment) in scientific laboratories, in industrial settings, and in the field.

Precision is critical in the design and fabrication of an electrostatic sector for a mass spectrometer. Especially notable is a very tight tolerance on the radii of the sector rails (the concentric cylindrical electrode surfaces); for this particular electrostatic sector, the nominal inner and outer radii are 29.21 and 30.48 mm, respectively, and the difference between these radii must not vary by more than 10 μm over the entire arc. In an older design, the two rails were fabricated separately, making it necessary to resort to an elaborate and laborious procedure to align them with each other to satisfy the radius requirement as well as to obtain the required precise alignment between these rails and the other spectrometer components. The older two-piece design also made it difficult to maintain alignment during transport. These difficulties of establishing and maintaining alignment added significantly to the cost of fabrication and limited use to applications in which ruggedness was not needed.

The improved electrostatic sector is inherently rugged and dimensionally stable because it is made from a single piece of a machinable ceramic. The electrodes are made by plating the machined concentric electrode surfaces with nickel to a thickness of 6 μm. Reference surfaces for alignment are machined onto the single piece of ceramic; these surfaces are designed to be positioned on alignment ridges on a mounting plate that is also a precise component of the mass spectrometer. Two screws hold the unitary electrostatic sector in place with the reference surfaces pressing against the alignment ridges. Thus, provided that the concentric electrode surfaces and the reference surfaces are machined within tolerances, alignment of the electrodes with the other components of the mass spectrometer is assured. As a result, the cost of fabrication is no more than about 1/40 of that of the older electrostatic-sector design.

This work was done by Mahadeva P. Sinha of Caltech for **NASA's Jet Propulsion Laboratory**. *Further information is contained in a TSP [see page 1].*

In accordance with Public Law 96-517, the contractor has elected to retain title to this invention. Inquiries concerning rights for its commercial use should be addressed to

Technology Reporting Office
JPL
Mail Stop 122-116
4800 Oak Grove Drive
Pasadena, CA 91109
(818) 354-2240

Refer to NPO-20215, volume and number of this NASA Tech Briefs *issue, and the page number.*

Materials

Hardware, Techniques, and Processes

BLANK PAGE

Protective Anode Separators for Rechargeable Lithium Cells

These separators would help protect against internal short-circuiting in overdischarge.

NASA's Jet Propulsion Laboratory, Pasadena, California

The anode separators in rechargeable lithium-ion electrochemical cells that contain carbon lithium-intercalating anodes with copper current collectors would be modified, according to a proposal, to give some protection against the internal short-circuiting that tends to occur during overdischarge. The carbon anodes offer advantages of greater safety and chemical stability over anodes made of pure lithium, but they also introduce a need to limit discharge, as explained below. The modified anode separators would not obviate the need to limit discharge, but would help to retard or prevent internal short-circuiting when overdischarge occurs despite efforts to prevent it.

In a cell that contains a pure lithium anode, there is still plenty of lithium left in the anode, even during overdischarge. However, in a cell with a carbon anode, no more lithium is available from the anode once discharge is complete. Therefore, during overdischarge, lithium ions are not being intercalated into the cathode; instead, a new electrochemical cell is formed between the cathode and the copper current collector in the anode. As overdischarge proceeds, copper is dissolved from the anode current collector and travels through the pores in the cell separator toward the cathode. Eventually, the deposited copper forms an electrically conductive path between the anode and cathode; that is, a short circuit develops within the cell.

The proposed modification of the separator in a given cell must be tailored according to the nonuniformity of utilization of the carbon electrode and of the distribution of electric current between the cathode and anode. In other words, it is necessary to identify the location on the carbon electrode that is most likely to be susceptible to short-circuiting during overdischarge. In a prototype cell, this location is an anode tab. The essence of the proposed modification is to render nonporous the part of the anode separator bag that covers the tab, to prevent penetration by copper.

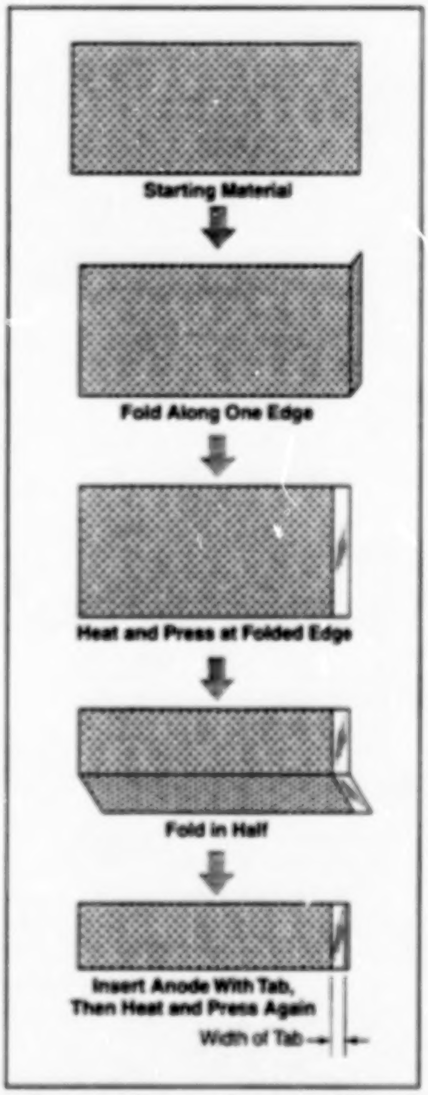

A Sheet of Porous Separator Material Would Be Formed into a separator bag with a nonporous, transparent edge in the tab region.

The figure illustrates how a modified separator bag for the prototype cell could be fabricated. The starting separator material would typically be a rectangular sheet of microporous polypropylene, which would be opaque because of its porosity. The sheet would be folded along one of the shorter edges, then pressed and heated to close the micropores. Upon closure of the micropores, the folded, pressed edge region would become transparent. The heating and pressing would also cause the two layers of the fold to merge into a single transparent layer. The reason for folding before heating and pressing is that a single layer of hot-pressed material could still contain holes that would allow penetration of copper, while a double layer has proved effective in preventing penetration of copper.

The sheet would be folded again — this time in half along its larger dimension to form a separator bag. The carbon anode could then be enclosed in the bag with the tab portion visible through the hot-pressed edge region.

This work was done by Chen-Kuo Huang of Caltech for **NASA's Jet Propulsion Laboratory**. *Further information is contained in a TSP [see page 1].*

In accordance with Public Law 96-517, the contractor has elected to retain title to this invention. Inquiries concerning rights for its commercial use should be addressed to

Technology Reporting Office
JPL
Mail Stop 122-116
4800 Oak Grove Drive
Pasadena, CA 91109
(818) 354-2240

Refer to NPO-19950, volume and number of this NASA Tech Briefs issue, and the page number.

Time-Dependent Nature of Adhesive EA946

Temperature and aging times affect the viscoelasticity of this adhesive.

Marshall Space Flight Center, Alabama

More accurate analyses of adhesive EA946 can now be accomplished using new mathematical models. Tests involving this adhesive (used in the space shuttle's reusable solid-rocket-motor nozzle and other rocket-motor nozzles) indicated that the adhesive is nonlinearly viscoelastic at short equivalent times and linearly viscoelastic at long equivalent times. These tests also showed that the material properties of EA946 change with aging time after cure.

The viscoelastic nature of EA946 was modeled using a strain-dependent time-shift factor. Aging effect with only a time-shift factor was also modeled. An assumption (from earlier test data) that the bulk modulus of this adhesive

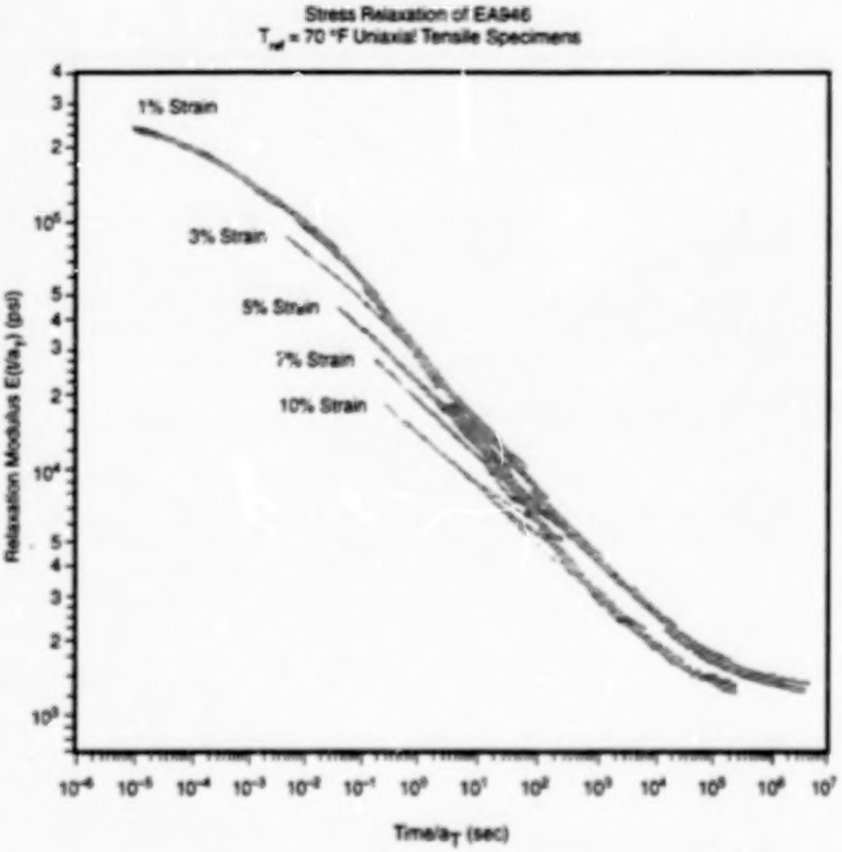

This mathematical model shows that Stress Relaxation Curves were divergent for short equivalent times and convergent for long equivalent times at 70 °F (21 °C).

remains constant for all times and temperatures was used for these modeling investigations.

During previous testing of this adhesive, master stiffness curves at various strain levels were recorded. The curves were generated from stress-relaxation data at a given strain level, using several different temperatures.

The figure illustrates how stress-relaxation curves of 1, 3, 5, 7, and 10 percent were divergent for short equivalent times and convergent for long equivalent times. Aging time after the cure caused the trend differences between the 1-percent and the 3-, 5-, 7-, and 10-percent stress-relaxation data.

Strain-shift and aging factors were added to the testing to account for the nonlinearities and aging effects. The temperature-shift factor was also introduced into the model.

After many attempts to model the material response of EA946 using a linear viscoelastic model, nonlinearities were introduced into the model. Shift factors that were a function of strain-level and time were used to evaluate the nonlinearities. This approach for evaluating the nonlinearity of adhesive EA946 accounted for the strain-level dependence of uniaxial tests (as noted in the illustration).

Tests showed the material properties of EA946 to be sensitive to the effects of age-time after cure. A series of additional aging tests conducted at 0 day, 1 day, and 3, 5, 10, 60, 90, and 365 days indicated that the elastic modulus increased 110 percent with 90-day aging and 370 percent with one-year aging. The ultimate strain decreased by approximately 75 percent, while the strength of the bulk adhesive did not appear to increase. Additionally, the bondline strength increased by approximately 25 percent during one year of aging.

This work was done by David E. Richardson and Russell A. Crook of the Thiokol Corporation for **Marshall Space Flight Center**. *Further information is contained in a TSP [see page 1].*
MFS-31161

Microwave Brazing of Polycrystalline Diamond Onto Drill Bits

Temperatures would be controlled to achieve brazing without overheating.

NASA's Jet Propulsion Laboratory, Pasadena, California

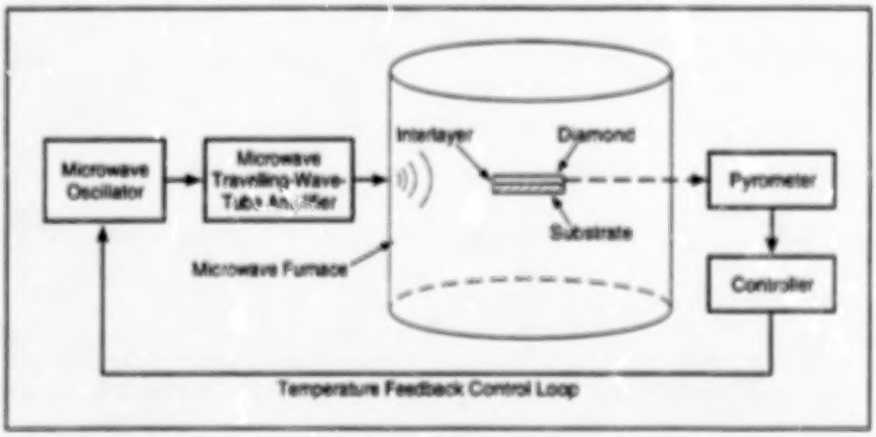

Microwave Heating with temperature feedback control makes it possible to braze polycrystalline diamond to an underlying layer of tungsten carbide, without overheating the diamond.

A microwave-heating technique has been developed for making a braze joint (1) between a tungsten carbide support and a surface layer of polycrystalline diamond or, alternatively, (2) between a tungsten carbide support and a relatively thin tungsten carbide backing layer with polycrystalline diamond on its working surface. The technique would be used to fabricate diamond-covered cutting tool bits. Such bits could be used, for example, to drill geothermal wells and would be improved versions of some of the diamond-covered bits now used to drill oil and gas wells. Whereas the braze joints of the oil-and-gas-well versions become weakened at temperatures ≥ 700

°C, the braze joints of the improved drill bits would be designed to withstand hard-rock-drilling temperatures up to 900 °C.

The major problem in fabricating the improved drill bits is to use higher-melting-temperature brazing materials and to heat the braze joints accordingly to effect brazing, without overheating the diamond. "Overheating" in this context means heating to a temperature ≥ 1,200 °C, causing the diamond to become graphitized and thereby to lose resistance to wear. The basic idea of this technique is to utilize the selective heating characteristics of microwaves to develop the required brazing temperature without overheating the diamond. Selective heating would be possible because the commercially fabricated diamond is a very good absorber of microwaves, while the proposed brazing materials would be moderate to good absorbers.

The proposed microwave-technique is related to microwave-heating techniques described in two prior articles in *NASA Tech Briefs*; "Selective Microwave Heating of Thin-Film Heterostructures" (NPO-19402), Vol. 21, No. 3 (March 1997), page 16a and "Microwave-Induced Combustion Synthesis of Ceramic/Metal Composites" (NPO-19637) Vol. 21, No. 5 (May 1997), page 26. The temperature of the layer of brazing material ("braze interlayer") in a given case would depend on the microwave energy absorbed, on conductive and radiative transfer of heat between this layer and the adjacent substrate and diamond layers, and on thermal radiation from the diamond surface layer to free space.

Experience teaches that the best capillary action and shear strengths in braze joints on diamond/tungsten carbide tool bits are achieved with fillets of 0.08 to 0.8 mm, and that braze interlayers should be thick enough (at least 0.02 mm) to relieve stresses caused by differential thermal expansion between diamond and tungsten carbide. The brazing material must be able, at the brazing temperature, to wet or diffuse into both the diamond surface layer and the tungsten carbide substrate or into the tungsten carbide backing layer and tungsten carbide substrate, as the case may be.

In preparation for a typical fabrication process according to this technique, a diamond disk 2 to 3 mm thick is placed on top of a braze interlayer 0.08 to 0.8 mm thick on top of a tungsten carbide substrate. This assembly of components is mounted in a region of strong electric field in a microwave processing chamber. A pyrometer is focused on the diamond surface layer; during the subsequent microwave heating, the output of the pyrometer is used to monitor the temperature of the diamond, and is used as a feedback signal to control the microwave power to achieve the desired brazing temperature. The dimensions of the braze interlayer, the components to be brazed, and the process tooling are chosen, along with the temperature-vs.-time heating curve, to obtain the strongest possible braze joint with minimal residual stress from differential thermal expansion.

The braze interlayer could consist of a foil of a braze filler metal. Alternatively, the braze interlayer could be made of a combustion-synthesis compound, in which case microwave heating would be used to ignite a combustion wavefront with temperatures of thousands of degrees. When this wavefront reached the interfaces with the adjacent backing and substrate layers, it would provide sufficient local heating to form the desired braze joint.

This work was done by Martin Barmatz and Henry W. Jackson of Caltech and Robert P. Radtke of Technology International Inc. for **NASA's Jet Propulsion Laboratory**. *Further information is contained in a TSP [see page 1].*

In accordance with Public Law 96-517, the contractor has elected to retain title to this invention. Inquiries concerning rights for its commercial use should be addressed to

Technology Reporting Office
JPL
Mail Stop 122-116
4800 Oak Grove Drive
Pasadena, CA 91109
(818) 354-2240

Refer to NPO-20080, volume and number of this NASA Tech Briefs *issue, and the page number.*

BLANK PAGE

Computer Programs

BLANK PAGE

These programs may be obtained from COSMIC. Please contact
COSMIC®
Computer Services Annex
University of Georgia
Athens, GA 30602
Telephone No. (404) 542-3265.

Mechanics

Software for Analysis and Design of Turbomachinery Seals

These programs can be used to design seals to improve overall machine performance.

Several computer programs, denoted collectively as the "CFD Seal Analysis Industrial Codes," have been developed to enable rapid parametric analyses and optimization of designs of a variety of turbomachinery seals. These programs could be used to design the seals that will be needed in future air-breathing and other aerospace systems, with improvements to enhance efficiency, prevent leakage, control flows of lubricants and coolants, prevent the entry of contaminants, inhibit mixing of incompatible fluids, and assist in controlling dynamic responses of rotors.

One of the programs is GCYL (Gas Cylindrical Seals), which can be used to analyze a variety of cylindrical seals, including ones with steps, tapers, and hydrostatic geometries. This code is a Reynolds-equation solver that accommodates laminar and turbulent flows in the film region. This code is principally applicable to seals with low-clearance geometries; for example, floating ring and circumferential sectored seals. This code computes clearance and pressure distributions, leakage, interface loads, righting moments, viscous dissipation, and frequency-dependent coefficients of stiffness and damping. Plotting routines are also provided to aid the visualization of clearance and pressure distributions. This code can be applied to seals for compressors, industrial gas turbines, and jet engines. It has also been applied to helium buffer seals for cryogenic pumps.

The Gas Face Seals (GFACE) program is similar to GCYL except that it applies to face geometries.

The Spiral-Groove Gas Seals (SPIRALG) program can be used to analyze spiral-groove, cylindrical, and face seals. Spiral-groove seals are becoming widely used in gas compressors, gas circulators, and computer disk drives. In SPIRALG, flow is assumed to be laminar and isothermal and to take place in narrow grooves. SPIRALG computes forces, moments, film thicknesses, leakage, power losses, and cross-coupled, frequency-dependent stiffness and damping coefficients.

The Spiral-Groove Liquid (Incompressible) Seals (SPIRALI) program is based on Hir's bulk-flow model with the addition of spiral-groove theory. Turbulence is treated with an extended form of Hir's bulk-flow model, generalized to include separate and arbitrary friction-factor Reynolds-number relationships for each surface. Film inertia is treated globally. Narrow-groove theory is used to characterize spiral grooves, maintaining the global representation. For geometries with film discontinuities (for example, with parallel and multiple helical grooves), loss coefficients are used. Effects of rough surfaces can also be modeled by applying friction-factor relationships. As in the case of SPIRALG, the output of SPIRALI includes forces, moments, film thicknesses, leakage, power losses, and cross-coupled, frequency-dependent stiffness and damping coefficients. One can also use SPIRALI to analyze pressure-breakdown bushings, wearing rings, and damping seals for high-pressure pumps and cryogenic turbomachines.

The Liquid (Incompressible) Cylindrical Seals (ICYL) program affords capabilities for analyzing two-dimensional, incompressible, isoviscous, turbulent flow in a cylindrical geometry; rotation of a rotor and/or a housing; roughness of both the rotor and the housing; and inertial pressure drops at inlets to fluid films from the ends of a seal and from pressurized pockets. Inertial effects are incorporated by applying a Bernoulli relation at each boundary point and reducing the static pressure by the computed kinetic-energy density. Capabilities for modeling Couette and Poiseuille flow, turbulence, and cavitation are included. Such geometric features as steps, pockets, tapers, preload arcs, and hydrostatic recesses can be treated. ICYL computes pressure and clearance distributions, rotor position, forces, moments, pocket pressures and flows, and cross-coupled coefficients of stiffness and damping. Plotting routines are included in ICYL. Applications for ICYL include liquid hydrostatic and hydrodynamic seals for pumps, cryogenic machines, and miscellaneous machinery.

The Liquid (Incompressible) Face Seals (IFACE) program is similar to ICYL, except that it applies to face seals rather than to cylindrical seals.

The Knife-to-Knife Analysis of Labyrinth Seals (KTK) program computes leakages and distributions of pressure through labyrinth seals. Applications include all gas-seal turbomachinery. Both straight-through and step labyrinths are considered. Input data are required to describe the geometry of a seal and the environmental conditions that affect leakage. Output is provided in the form of flow and flow-resistance characteristics; for example, flow factor versus pressure ratio. An optimization feature included in the program enables the user to identify global geometric constraints and enables the program to identify an optimum seal configuration based on minimum leakage.

The Dynamic Response of Seals (DYSEAL) program determines the tracking capabilities of fluid-film seals and can be used to analyze effects of parametric variations in geometry to improve dynamic responses. This code can be used to analyze face seals and floating-ring cylindrical seals. In the case of a face seal, the rotating or mating ring can be treated as vibrating in five degrees of freedom — translations along three Cartesian axes (x, y, and z) and rotations about two of these axes (x and y). The response of the seal ring is also modeled in five degrees of freedom. The interface is represented by cross-coupled stiffness and damping coefficients obtained from other programs. The effects of Coulomb friction of secondary seals on the seal-ring response are included. Input options for piston-ring and O-ring secondary seals are provided. The floating-ring-analysis portion of this program accommodates two degrees of freedom for both the seal and the ring, and is intended to determine the response of the ring to an orbiting shaft. A secondary seal occurs between a ring and a wall, and the x-y Coulomb friction there is taken into account. The general method of computation is a forward integration in time that yields absolute motions in all degrees of freedom. At every time step, friction must be evaluated to determine whether motions continue or are halted.

A graphical user interface (GUI) program couples the aforementioned programs through system executive software. Input is prepared with the help of menus, dialogue boxes, and button options, in a manner similar to that of the Windows operating system prevalent in contemporary personal-computer usage. Input files can be prepared manually by use of text-editor software, and the instructions for doing so are included in the technical manuals for the individual programs.

The CFD Seal Analysis Industrial Codes collection is written in FORTRAN 77 for IBM-PC-compatible computers running the OS/2 operating system. A random-access memory of at least 8MB is recommended. A computer based on an 80386 or 80486SX processor must include a math coprocessor. Executable code is provided. The software has been successfully implemented on '486-class IBM personal computers with version 2.1 (and more recent versions) of the OS/2 operating system. Source code can be compiled on such other operating systems as Windows 95 or Windows NT. A Watcom FORTRAN 77 compiler is necessary for compiling this software. The GUI will be available under OS/2 only. The standard distribution medium is a set of nine 3.5-in. (8.89-cm), 1.44MB MS-DOS-format diskettes. The CFD Seal Analysis Industrial Codes collection was released to COSMIC in 1997.

This program was written by W. Shapiro, B. B. Aggarwal, J. Walowit, and A. F. Artiles of Mechanical Technology, Inc., for **Lewis Research Center***. The KTK program was written by R. E. Chupp, G. F. Holle, and T. E. Scott of Allison Gas Turbine, a division of General Motors Corporation, and was included in the CFD Industrial Codes with the permission of the U.S. Air Force.*

Further information is contained in a TSP [see page 1].
LEW-16582

Mathematics and Information Sciences

Generic Graphical-User-Interface Program for FORTRAN Input

A custom user interface is generated from information about namelist input variables.

The NLEDIT computer program implements a generic graphical user interface for the preprocessing of FORTRAN namelist input files. The interface consists of a menu system, a message window, a help system, and data-entry forms. A form is generated for each namelist. The form includes an input field for each namelist variable along with a one-line description of that variable. Detailed help information, default values, and minimum and maximum allowable values can all be displayed via menu picks. Inputs are processed through a scientific-calculator program that provides for the use of complex equations instead of simple numerical inputs. A custom user interface is generated simply by entering information about the namelist input variables into an ASCII file. There is no need to learn a new graphics software system or programming language. NLEDIT can be used as a stand-alone program or as part of a larger graphical-user-interface program. Although NLEDIT is intended for files using namelist format, it can be easily modified to handle other file formats.

NLEDIT is customized for a particular application by use of a data-definition file. The data-definition file is an ASCII file that contains such information about such program inputs as the names, types, dimensions, default values, and limits of variables, plus help information. NLEDIT reads this information into a data base and then uses it to produce an appropriate interface. The user interface changes only in appearance for a particular data-definition file; no recompiling of code is necessary.

The NLEDIT Program is composed of three main modules: the calculator module, the data dictionary (or data base), and the graphics module. The calculator module is used to convert an equation, in the form of a character string, into a numerical value. The data dictionary allows the other modules to store and retrieve information about specific items defined in the data-definition file. The graphics module is the Motif code for displaying windows and processing input events.

NLEDIT is written in C language and has been successfully implemented on an SGI Indigo 2 computer under IRIX 5.3, an IBM RS/6000 computer running AIX v4, and a Sun Sparcstation computer under SunOS 4.1.3. This software package requires MIT's X Window System, Version 11, Revision 4 and OSF/Motif 1.1 or higher. A FORTRAN 77 compiler that supports namelist input is also required to compile the included sample FORTRAN program. The standard distribution medium for NLEDIT is a 0.25-in. (6.35-mm) streaming-magnetic-tape cartridge (Sun QIC-24) in UNIX tar format. Alternate distribution media are available upon request. An electronic copy of the documentation in PostScript format is included on the distribution medium. NLEDIT was released in 1995.

This program was written by B. P. Curlett of **Lewis Research Center***. Further information is contained in a TSP [see page 1].*
LEW-16141

Mechanics

Hardware, Techniques, and Processes

BLANK PAGE

Manipulation of Liquids by Use of Sound: Part I

Liquids and objects suspended in liquids could be manipulated nonintrusively.

Lewis Research Center, Cleveland, Ohio

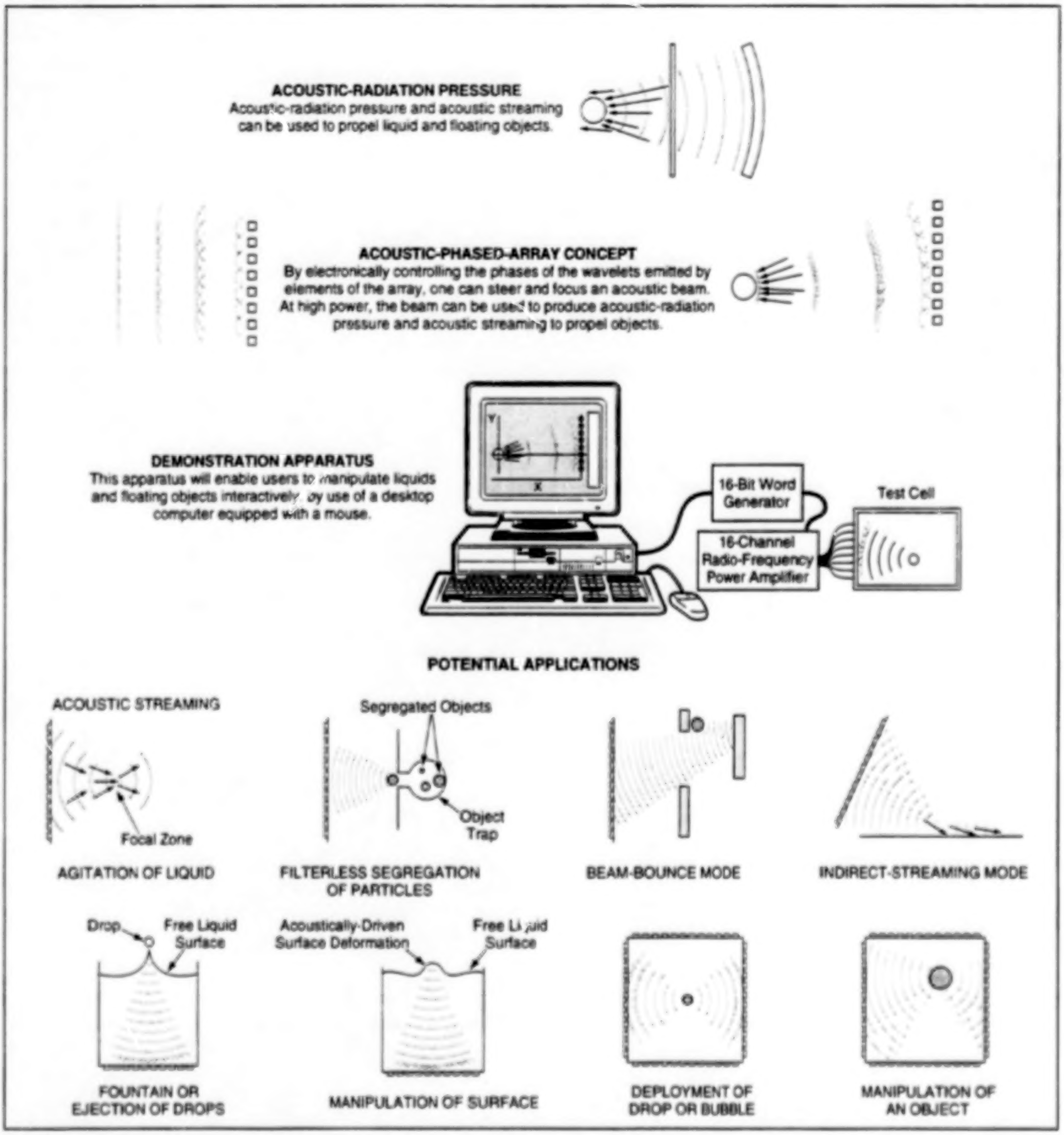

The **Acoustic-Phased-Array Concept**, similar to the concept of phased-array antennas for electromagnetic waves, involves the exploitation of collective effects of waves emitted by elements of an array. Here, acoustic (instead of electromagnetic) beams are steered and focused by controlling the phases of excitations applied to the elements of the array.

An acoustic-radiation-pressure phased array (ARPPA) is undergoing development at Lewis Research Center. ARPPAs are envisioned as general-purpose, nonintrusive tools for manipulating both liquids and objects suspended in liquids.

Acoustic-radiation pressure and acoustic streaming are effects created by high-intensity sound. Acoustic-radiation pressure applies forces to objects situated on acoustic paths. Acoustic streaming is a unidirectional flow that can arise because sound can exert a thrust on a liquid in which it propagates. ARPPAs would make it possible to exploit acoustic-radiation pressure and acoustic streaming (see figure) to perform such manipulation and control functions as

propelling or agitating liquids, moving floating objects, controlling the shapes of liquid surfaces, or ejecting liquid drops.

A beam of sound can be produced by use of an array of acoustic transducer elements. Each element emits small wavelets of sound that, over a distance, overlap other wavelets. Wavelets that are in phase tend to coalesce into a single beam. If the wavelets are focused, then their amplitudes become superimposed to form a beam of high intensity. The distinguishing feature of an ARPPA is that one can electronically control the phase relationships among the elements of the array to steer the beam and adjust the size and shape of the focal region. Thus, one can adjust the position and shape of the region where acoustic-radiation pressure and acoustic streaming occur.

An interactive-computer-controlled ARPPA demonstration apparatus is under construction. This apparatus is designed to enable a user to interactively control the focus and position of an acoustic-radiation-pressure beam. The apparatus is expected to aid in the development of specific users' applications.

An ARPPA enables a user to exert some control over a liquid without intruding into its container. ARPPAs might be capable of performing the functions of such other mechanical devices as agitators, filters, probes, and manipulators. The ARPPA approach holds promise for simplifying systems by reducing the need for external plumbing and intrusive mechanisms and for such high-maintenance items as seals and bearings.

Potential uses for ARPPAs include the following:

- Agitation of Liquids: ARPPAs could provide the agitation needed for processes that involve liquids in sealed systems. ARPPAs could be used to disperse accumulations of particles, and to form and maintain such suspensions as slurries, paints, and pastes. Furthermore, agitation of liquids by use of acoustic-radiation pressure could be used to obliterate thermal gradients or concentration gradients and thereby prevent stratification of chemicals in vessels.
- Segregation of Gas Bubbles and Solids Suspended in Liquids: ARPPAs might be useful for segregating objects suspended in liquids in sealed systems, without using filters. Acoustic-radiation pressure could be used to force contaminant bubbles and particles into traps, where they could be rendered harmless without breaking into the system. The elimination of in-line filters would reduce probabilities of clogging and reduce the amount of maintenance needed, and could thus also be useful in reducing the risk of contamination of the environment from systems that process toxic chemicals.
- Ejection of Liquid Drops: If droplets could be ejected from a pool of liquid without using a nozzle, then there would be no risk of clogging. Therefore, suspended particles would not hinder operation. By use of acoustic-radiation pressure with precise focus combined with tone-burst control, one could eject drops on demand, with precise control of sizes and velocities of the drops. One could use acoustic-radiation pressure in this way to dispense picoliter volumes of liquids on demand, to apply paints or other liquid coating materials without using masks, or to apply molten metals (e.g., solder in automated soldering of circuit boards).
- Manipulation of Free Surfaces: ARPPAs could be used to control surface waves for such purposes as suppression of sloshing or of standing waves in tanks. Surfaces could be manipulated to control wetting through selective forcing of liquids into contact with solid surfaces. Solder fountains driven by acoustic-radiation pressure might be useful as means to refine the common wave-soldering method used to solder electronic-circuit boards. ARPPAs could also be used to drive surface waves on liquids for the selective application of adhesive and other coating materials.
- Manipulation of Immersed Objects: ARPPAs could be used to manipulate such immersed objects as bubbles, drops of immiscible liquids, or partially buoyant solid objects. The focusable, steerable nature of ARPPAs could be used to move such objects though complex paths and even to oppose such forces as those associated with gravitation, fluid currents, and electromagnetic fields. ARPPAs could be employed to orient and concentrate fibers and other reinforcing constituents to be cast in composite structures. In outer space, ARPPAs could control the ingestion of gas bubbles into tanks containing liquids. ARPPAs might be useful for micromanipulation of biological tissues in liquid media. ARPPAs might even be proven suitable for nonintrusive repositioning of detached retinas human eyes.

This work was done by Richard C. Oeftering of **Lewis Research Center**. *Further information is contained in a TSP [see page 1].*

Inquiries concerning rights for the commercial use of this invention should be addressed to NASA Lewis Research Center, Commercial Technology Office, Attn: Tech Brief Patent Status, Mail Stop 7–3, 21000 Brookpark Road, Cleveland, Ohio 44135. Refer to LEW-16470.

Manipulation of Liquids by Use of Sound: Part II

Drops and bubbles could be controlled with minimal equipment.

Lewis Research Center, Cleveland, Ohio

Acoustic-radiation pressure can be used to improve performance in the dispensing of liquid drops into gases or vacuum and in dispensing gas bubbles into liquids. In a typical application involving dispensing a liquid, this is accomplished by use of a high-frequency, high-intensity acoustic transducer coupled with a conventional syringe and hollow dispensing needle (similar to a hypodermic needle). A small dose of liquid passes through the needle and forms a drop at the tip. The drop is held in place by surface tension. The acoustic transducer emits a premetered acoustic tone burst at high power. The bore of the needle conducts the acoustic waves to the drop, where acoustic-radiation pressure creates a force on the droplet. When the burst of force is sufficient to overcome surface tension, the drop separates from the tip.

Unlike in previous approaches to dispensing, it is not necessary to rely on gravitation or on the inertia of drops to cause deployment. Usually, the sizes of drops are proportional to the sizes of needles, but by use of acoustic-radiation pressure, one can deploy drops independently of needle sizes. Because deployment by acoustic-radiation pressure is controlled electronically, it is possible to adjust the acoustic excitation to deploy or dispense drops of various liquids and various sizes with various initial velocities, on command.

In a given apparatus, acoustic waves can be coupled from a transducer in any of

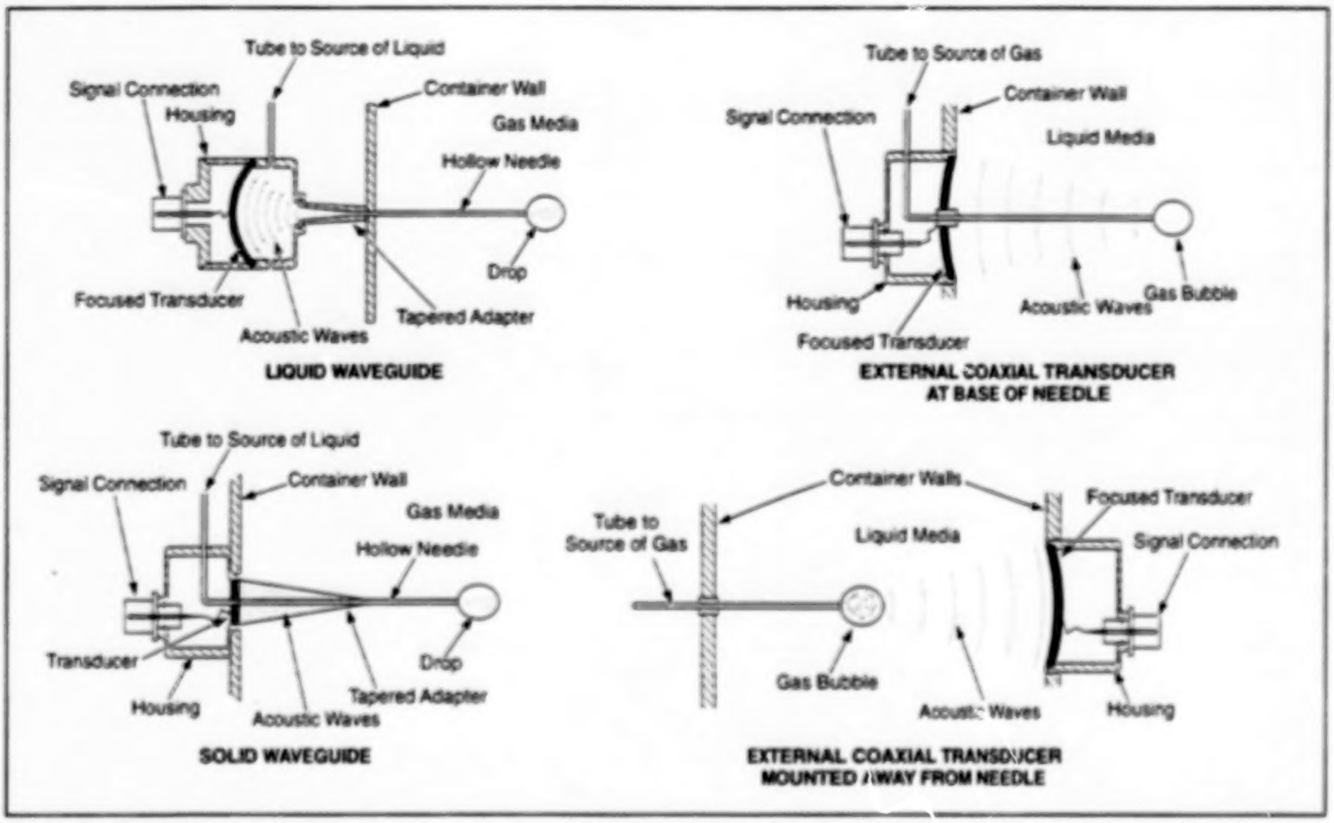

These Are Examples of Schemes for coupling acoustic waves from a transducer to a liquid drop or a bubble to be dispensed from the tip of a hollow needle.

several schemes. Examples (see figure) include (1) using the fluid in the bore of the needle as a waveguide to conduct acoustic power to the drop at the tip of the needle; (2) using an external coaxial transducer mounted at the base of the needle and focused at a bubble at the tip of the needle; (3) using the cylindrical wall of the needle as a solid waveguide to conduct the acoustic waves from transducer to the drop at the tip; or (4) using an external coaxial transducer mounted away from the needle and focused at a bubble at the tip. The fourth-mentioned scheme is suitable for the case in which a bubble does not stick to the needle; the acoustic transducer in this scheme emits an opposing acoustic beam that pins the bubble in place until it is time to release the bubble on command. All of the foregoing schemes can be used individually or in combination.

Acoustic transducers can also be used as sensors. One can exploit this sensory capability to measure positions of drops and bubbles. By monitoring the electrical signal from a transducer, one can verify deployment of a drop or bubble, without visual monitoring of the drop or bubble.

Potential applications in which one could use acoustic-radiation pressure to enhance dispensing of drops and bubbles include the following:

- Outer-Space Applications: Specific applications include fluid-physics, drop-physics, and droplet-combustion experiments; containerless processing; and dispensing liquids in a variety of systems in which premetered drops are needed.
- Terrestrial Applications: The behaviors of drops and bubbles could be controlled while using fewer mechanical parts and less plumbing than are now needed for such purposes. Such control could be exploited for precise placement of paints, dyes, adhesives, liquid coating materials in general, pastes (including slurry pastes), and molten solders used in manufacturing. In many applications, this acoustic-radiation-pressure approach could eliminate the need for masks and related tooling and processing. This approach can also be followed in precise dispensing of drops and bubbles in chemical processes and in medical applications.

This work was done by Richard C. Oeftering of **Lewis Research Center**. *Further information is contained in a TSP [see page 1].*

Inquiries concerning rights for the commercial use of this invention should be addressed to NASA Lewis Research Center, Commercial Technology Office, Attn: Tech Brief Patent Status, Mail Stop 7-3, 21000 Brookpark Road, Cleveland, Ohio 44135. Refer to LEW-16469.

Designing With Help of Neural-Network and Parallel Computing

Large design problems can be solved faster and more efficiently than before.

Lewis Research Center, Cleveland, Ohio

Structural Analysis/Design (STRAND) and Neural Net Computation (NETCOM) are developmental modular computer programs that exploit the speedup afforded by parallel and neural-network computing to drastically reduce the computation time needed to solve large design-optimization problems. These programs were originally intended for use in designing aerospace structures, but, when fully developed, will also be useful for optimizing designs of diverse nonaerospace structures, includ-

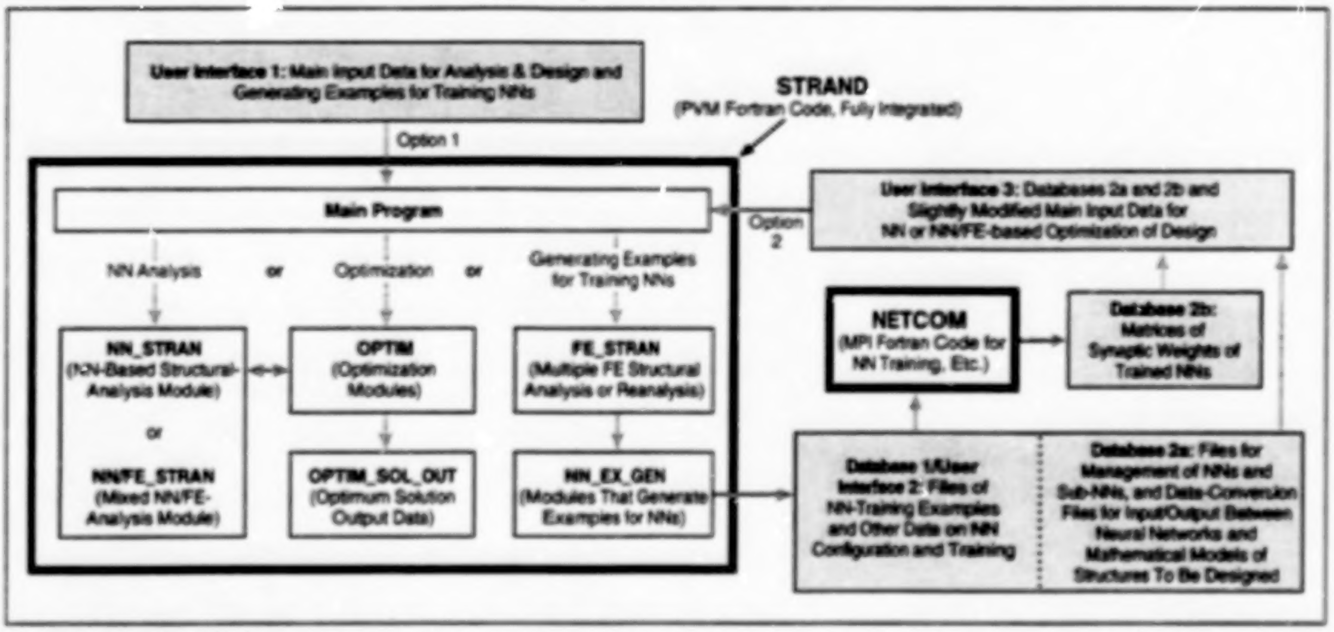

The **PAR_STRAND_NET Software System** utilizes a combination of neural-network, finite-element, stochastic-optimization, and parallel-computation techniques to reduce the computation time needed to solve large design-optimization problems.

ing high-rise buildings, automobile structures, and civil infrastructures.

STRAND and NETCOM have been integrated into PAR_STRAND_NET, which is a self-contained software system that can be implemented on either PVM or MPI standard networked parallel clusters of computer workstations and IBM SP computers. The figure shows the macro flow chart of PAR_STRAND_NET.

STRAND can perform automated design-optimization computations based on neural-network (NN), finite-element (FE), and mixed NN/FE analysis methods. STRAND affords computational capabilities to perform tasks as follows:

- Multiple concurrent structural analyses can be performed by use of parallel multiple FE and/or NN analysis methods and modules.
- Parallel optimization of structural design can be accomplished by use of FE and/or NN structural-analysis modules and an optimization module. The module implements the Integral Global /Local Optimization (IGLO) algorithm, which performs stochastic global and local searches. Built-in objective functions of structural weight, strain energy, and maximum displacement are used in optimization.
- Training examples and data bases for training neural networks can be created by use of concurrent multiple FE structural-analysis modules and a scaled-training-example data-reduction module.

NETCOM is capable of training multiple NNs or sub-NNs in parallel and of predicting NN output quantities by use of trained NNs. Training in NETCOM is effected by the back-propagation algorithm. A capability for concurrent training of multiple NNs or sub-NNs can be utilized in cases in which (1) the NNs or sub-NNs share the same input vector (typically, the same set of cross-sectional areas of structural members or of other design variables) but (2) the NNs or sub-NNs generate different output vectors (e.g., displacement vs. stress vectors) or numerically differing components of the same output vector. Once NN training has been completed, NETCOM generates a second data base that contains the matrices of synaptic weights of the trained NNs.

The use of NNs to replace FE reanalysis in the optimization of a structural design can reduce computational time by nearly an order of magnitude — an important advantage in the case of a large-scale design. Ordinarily, this advantage would be offset by the tedious and time-consuming nature of NN training. However, in this system, computational burden of NN training is reduced by the use of reduced NN models plus the efficient parallel and NN computational capabilities of NETCOM.

On the basis of numerical performance in tests conducted thus far, the IGLO algorithm was found to be much more efficient than are such other stochastic algorithms as those of the genetic and simulated-annealing types. Thus, it appears that IGLO offers great potential for solving large-scale design problems that involve not only continuous design variables but also discrete variables and mixes of continuous and discrete variables.

One likely goal of future development efforts would be to secure the advantages while avoiding the disadvantages of both gradient-based optimization (GBO) methods and stochastic methods like those of IGLO. GBO methods are inapplicable to mixed- and discrete-variable problems, and sometimes yield solutions that are not optimum in the sense that they correspond to local minima that differ from global minima of objective functions in design-variable space. On the other hand, whereas stochastic methods yield global solutions for continuous, discrete, and mixed variables, much more computation time is needed to find a local minimum in a stochastic method than in a GBO method. Therefore, it appears desirable to replace the continuous-local-search portion of the IGLO algorithm with a GBO algorithm to form an integrated IGLO/GBO algorithm to increase computational efficiency and the quality of solutions of problems that involve continuous, discrete, and mixed variables.

This work was done by Rong C. Shieh of MRJ Technology Solutions for **Lewis Research Center**. *Further information is contained in a TSP* *[see page 1].*

Inquiries concerning rights for the commercial use of this invention should be addressed to NASA Lewis Research Center, Commercial Technology Office, Attn: Tech Brief Patent Status, Mail Stop 7–3, 21000 Brookpark Road, Cleveland, Ohio 44135. Refer to LEW-16601.

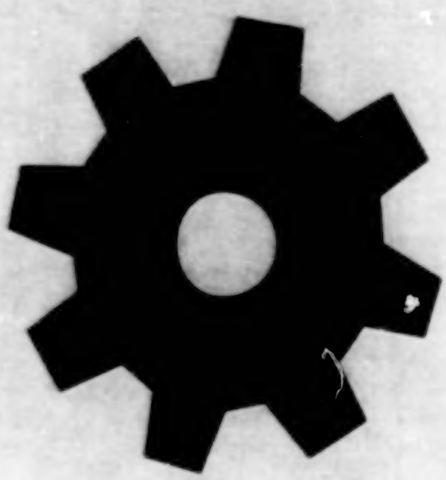

Machinery

Hardware, Techniques, and Processes

BLANK PAGE

Automated Propellant-Blending Machine

Production processes are faster and safer than before, and the product is improved.

Lyndon B. Johnson Space Center, Houston, Texas

The automated propellant-blending machine, a Johnson Space Center (JSC) innovation, refines the production processes of commercial rocket-propellant manufacturers by: (1) generating inert blends that contain particles of uniform size; (2) eliminating manual mixing, thereby speeding production and reducing the risk of injury or death; and (3) making it possible, with little or no modification, to produce a finer end-product for commercial and aerospace applications. These refinements are achieved by use of a nonproprietary technique — a significant departure in that commercial propellant manufacturers frequently use proprietary precipitation-drop techniques unavailable to other propellant manufacturers. One manufacturer has already expressed interest in the JSC automated propellant-blending machine.

Propellant-blending machines blend zirconium/potassium perchlorate (ZPP), titanium and titanium hydride propellants, and aluminum and magnesium compositions. Two commercial methods for blending ZPP are the evaporation method and precipitation blending. The disadvantages associated with the evaporation method are that the achievement of good blends depends upon, among other things, manual and frequent movement of mixtures, and production of the blends is dependent on the blender. Moreover, evaporation blending is dangerous; lives and limbs have been lost because of hazards associated with the blending process. The major disadvantage of precipitation blending is the unreliability of the process. The JSC automated propellant-blending machine overcomes the disadvantages of both evaporation and precipitation blending.

The JSC machine (see figure) includes a mixing container and a pouring container. An explosion-proof motor is connected by a shaft to an impeller (the blending actuator) in the mixing container.

In preparation for the blending process, a fluoroelastomer (Viton B or equivalent) is dissolved in acetone in proportions of 1:1, and the resulting solution is allowed to sit for a minimum of 24 hours. A required amount of hexane (which serves as a counter-solvent as explained below) is measured and put into a hexane fill container. The fluoroelastomer/acetone solution and the hexane are put into mixing container. The active ingredients of the propellant mixture are placed in the pouring container. These ingredients include the following: (1) zirconium and graphite, which are placed on one side of the pouring container, and (2) potassium perchlorate, which is placed on the other side. At this juncture, personnel leave the machine, and the automated propellant-blending process is begun.

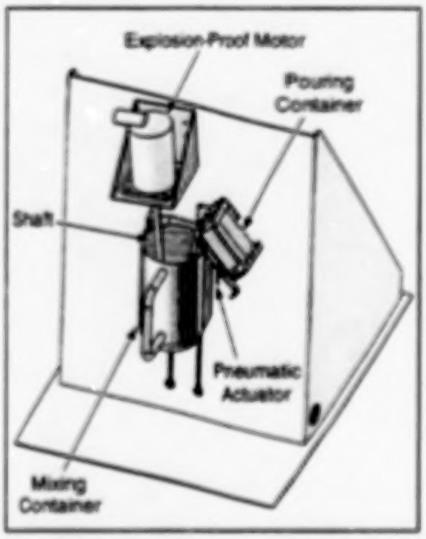

The JSC Automated Propellant-Blending Machine is a product of continuing efforts at JSC to study and apply processes for blending ZPP into propellant mixtures.

During this process, the operation of the automated blending machine is controlled by a program executed on a personal computer. The program activates the explosion-proof motor, which rotates the shaft/impeller assembly. The program also activates a pneumatic actuator that tilts the pouring container to pour the active propellant materials into the acetone/hexane/fluoroelastomer solution in the mixing container.

A solenoid valve is opened to add hexane, and the amount of hexane added is measured. When the hexane-to-acetone ratio exceeds a certain value, the fluoroelastomer starts to precipitate from the solution and to coat the particles of the active propellant material. The desired amount of hexane to be added is the amount needed to precipitate the desired amount of the fluoroelastomer. Once the desired amount of hexane has been added, the solenoid valve is closed. After about 1 minute of mixing with the desired amount of hexane present, the computer tells the motor to stop. A ball valve opens, and the acetone/hexane solution is siphoned from the mixing container and deposited in an acetone/hexane disposal container. The ball valve is then closed.

The solenoid valve is opened and closed so that hexane can be added to the coated active ingredients. The computer orders the motor to rotate at a high speed for about 1 minute. The motor is then stopped and the ball valve is opened so that the hexane solution can be siphoned into the acetone/hexane disposal container. The mixing container is removed from the machine and the mixture is poured into a U.S. standard no. 30 sieve submerged in counter-solvent. The sieved particles are dried in air at room temperature, then sent to an oven for final drying.

The automated process as described above is superior to the evaporation method or to precipitation blending in the following respects:

- The human factor is removed; this means that the blend is uniform and consistent, time is saved, the cost of producing the propellant mixture is reduced.
- The automated part of the propellant-blending process can be controlled remotely; this makes the process a lot safer by limiting the exposure of personnel.
- The speed of production is increased. As a consequence, the product can be delivered in a more timely fashion. Excluding drying time, one station can produce 400 g/hr.
- The mixing step is safer because the materials are not taken to dryness.
- The end-product is a loose powder that is much finer; this reduces the screening requirement.

This work was done by Paul Kemp, Carl Hohmann, and Maureen Dutton of **Johnson Space Center**; *Bill Tipton, Jr., of Lockheed Martin; and Jim Bacak of G. B. Tech. No further documentation is available.*

This invention is owned by NASA, and a patent application has been filed. Inquiries concerning nonexclusive or exclusive license for its commercial development should be addressed to the Patent Counsel, Johnson Space Center, (281) 483-0837. Refer to MSC-22757.

Miniature Joule-Thomson Rankine-Cycle Refrigerators

A two-stage refrigerator should be able to cool from 313 to 70 K.

NASA's Jet Propulsion Laboratory, Pasadena, California

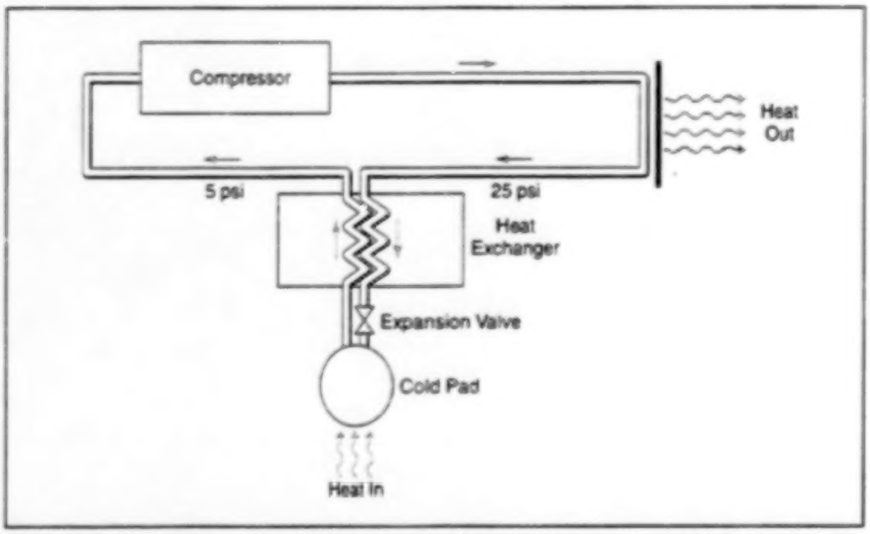

Schematically, a Single-Stage Refrigerator of the proposed type would look like an ordinary typical vapor-compression refrigerator. However, it would be fabricated in miniature, with a microperistaltic pump as its compressor. The working fluid would be a mixture of gases chosen for Joule-Thomson-cooling capability.

Miniature, lightweight, low-power, low-vibration Joule-Thomson Rankine-Cycle refrigerators have been proposed for cooling portable scientific instruments. These refrigerators would be made largely from silicon wafers by micromachining techniques like those used to fabricate integrated circuits. The compressors in these refrigerators would be microperistaltic pumps, in which voltages applied in spatial and temporal sequences to multiple electrodes positioned along channels would give rise to waves of electrostatic attraction that would cause membranes to pinch the channels closed at intervals in peristalsislike waves. [A fuller description of microperistaltic pumps was presented in "Microscopic Heat Exchangers, Valves, Pumps, and Flowmeters" (NPO-19093), *NASA Tech Briefs*, Vol. 22, No. 7 (July 1998), page 66.]

A single- or multiple-stage refrigerator according to this concept could be made from two fused wafers. The figure schematically illustrates a single-stage refrigerator, in which a microperistaltic pump would compress the working fluid (a mixture of gases as described below) from a lower pressure of 5 psi (34 kPa) to a higher pressure of 25 psi (170 kPa). The compressed fluid would flow along a microchannel, where it would be partly cooled by transfer of heat into the surrounding wafer material. Continuing along its flow path, the compressed fluid would be cooled further and condensed in the first of two microchannels in a highly thermally conductive counter-flow heat exchanger within the wafer. After leaving the heat exchanger, the fluid would flow along a microchannel to an expansion nozzle in a cold pad that is thermally well insulated except for contact with the object to be cooled.

Upon expansion in the nozzle, the fluid would evaporate, drawing latent heat of vaporization from the cold pad. The vapor would flow into the second microchannel in the heat exchanger, where it would absorb heat from the compressed fluid in the first microchannel. Upon emerging from the heat exchanger, the fluid would return to the lower-pressure port of the microperistaltic pump, completing the cycle.

The Joule-Thomson-cooling capabilities of a number of gas mixtures have been studied to assess their utility as working fluids for a refrigeration cycle between an exhaust temperature of 200 K and a refrigeration temperature of 70 K. One suitable fluid was found that consisted of nitrogen and five hydrocarbons. With a mass flow rate of 0.001 mole/second and a heat-exchange efficiency of 0.98, the refrigerator could handle a maximum heat load of 0.3 W while maintaining a temperature of 71 K.

For most terrestrial applications, it would be more practical to exhaust heat at a higher temperature, giving rise to the need for two stages of refrigeration to reach a low temperature of 70 K. For example, the first stage could exhaust heat at 313 K and provide cooling at 190 K, while the second stage would be like the single-stage refrigerator described above, with its exhaust heat removed by the cold pad of the first stage. The composition of a suitable working fluid for the first stage consisted of carbon tetrafluoride and miscellaneous hydrocarbons. With a mass flow rate of 0.001 mole/second and a heat-exchange efficiency of 0.98, the first stage could handle a heat load of 2 W while maintaining a temperature of 190 K.

This work was done by Frank T. Hartley and Jack A. Jones of Caltech for **NASA's Jet Propulsion Laboratory**. *Further information is contained in a TSP [see page 1].*

In accordance with Public Law 96-517, the contractor has elected to retain title to this invention. Inquiries concerning rights for its commercial use should be addressed to

Technology Reporting Office
JPL
Mail Stop 122-116
4800 Oak Grove Drive
Pasadena, CA 91109
(818) 354-2240

Refer to NPO-19956, volume and number of this NASA Tech Briefs *issue, and the page number.*

Fabrication Technology

Hardware, Techniques, and Processes

BLANK PAGE

Microgravity Fiber-Pulling Apparatus

This fiber-processing method provides a way to produce optical fiber composed of glass systems in microgravity.

Marshall Space Flight Center, Alabama

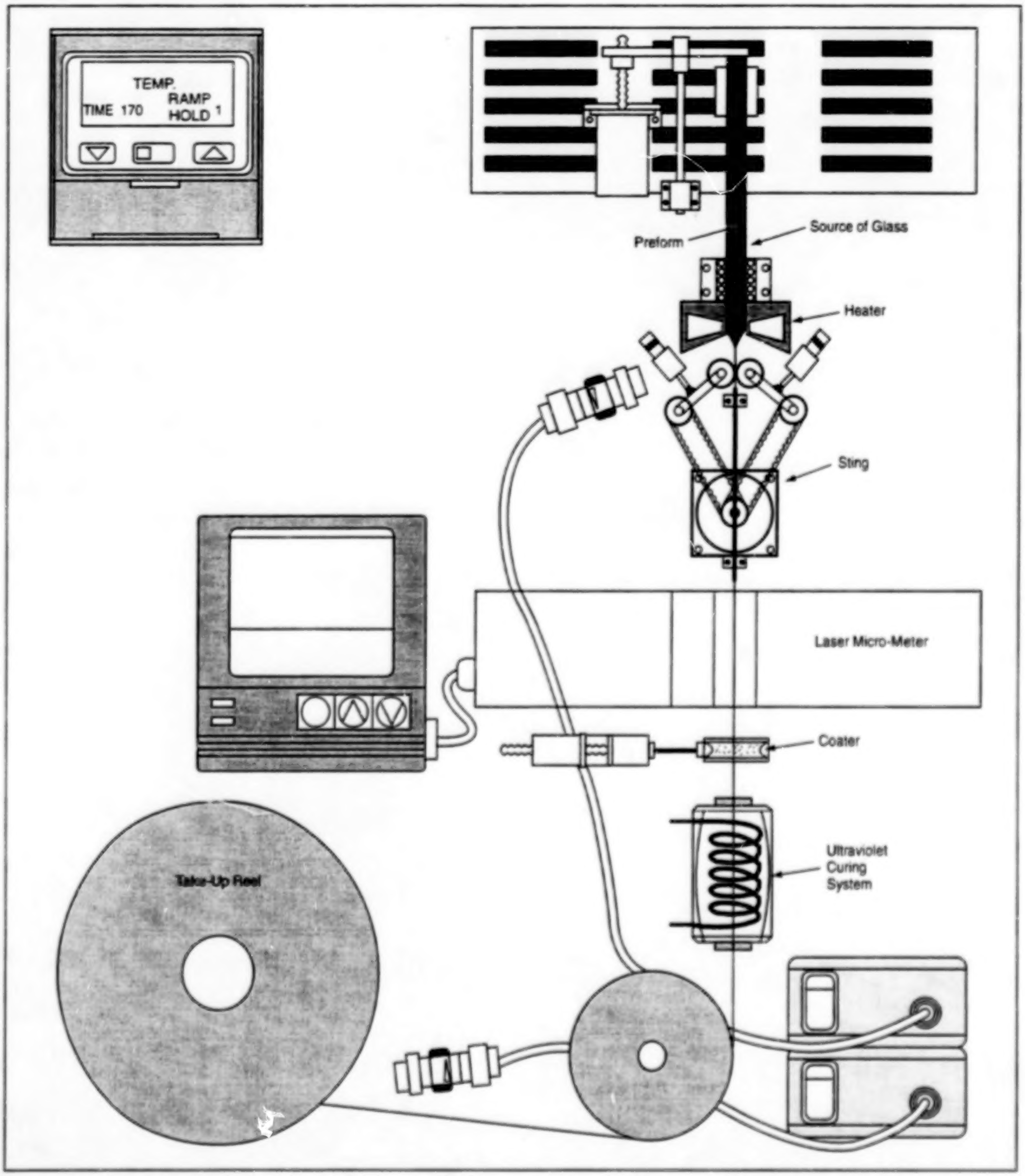

Components of the **Microgravity Fiber-Pulling Apparatus** include a source of glass (the preform), a sting to initiate the fiber-drawing process, a coating device, an ultraviolet curing system, and a take-up reel to place the fiber on after it has cooled.

A method to process optical fiber composed of glass systems has been developed in support of the space shuttle and Space Station programs. This process, known as the Microgravity Fiber-Pulling Apparatus, was designed to operate in a microgravity environment. It has the unique capability to produce heavy-metal glasses through the reduction of nucleation and allows low viscosity to be handled more easily. Optical fibers, such as the heavy-metal fluoride glasses, are usually very diffi-

cult to process in ground-based operations because the glass has inherent characteristics such as low viscosity, a narrow working range, and a tendency to form crystallites during processing.

Operation in microgravity has demonstrated that some of the conventional methods used in Earth-based fiber-forming processes will not function properly in a weightless environment. For example, the gravitational force necessary to initiate the fiber draw is not present in space. The components of this fiber-pulling apparatus include a source of the glass (preform), a sting to initiate the fiber-drawing process, a coating applicator for ultraviolet-curable cladding, an ultraviolet lamp, and a reel to place the drawn fiber on after it has been cooled. These components are shown in the figure.

Processing the glass system in microgravity is the most important step to forming more perfect fiber composed of the heavy-metal fluoride glasses. In microgravity, processing glass systems requires a sting (consisting of a platinum wire with a flat plate or fingers at the extremity) to pull molten glass out from the drawing aperture. Since current drawing chambers designed for space platforms do not allow extremely large volumes for fiber drawing, this design uses a chill block to quench the glass melt into a solidified fiber.

Another drawback to conventional methods of processing fiber is the coating applicator, which needs to be completely contained and have the ability to operate through a fluid-transfer line to provide uniform cladding on the fiber. A syringe-type or peristaltic pump provides this apparatus with the appropriate capacity and pressure.

This work was done by Dennis Tucker of **Marshall Space Flight Center** *and Gary Workman and Guy A. Smith of the University of Alabama in Huntsville. Further information is contained in a TSP [see page 1].*
MFS-26503

Mathematics and Information Sciences

Hardware, Techniques, and Processes

BLANK PAGE

Modular, Extensible Program Simulates Dynamics of Systems

This program lends itself well to analyses in which frequent changes of code are necessary.

Lyndon B. Johnson Space Center, Houston, Texas

The Multiple Object Orbital Dynamics Simulation (MOODS) computer program is a general, extensible, easily modifiable, and reusable software system for use in simulating the dynamics of such diverse engineering systems as aircraft, missiles, automobiles, industrial process-control systems, or other systems wherein time-dependent physical processes (e.g., unsteady chemical reactions) occur. MOODS contains a generic and reusable kernel, plus a large base of high-quality reusable primitives, utility subprograms, and models that assist it in rapidly prototyping extensions of itself and of other system-analysis application programs.

Among the components of MOODS are the following:

1. Primitive objects, mathematical types, and functions (vector, matrix, complex, and quaternion operators);
2. Statistical utilities (e.g., random-number generators);
3. Numerical methods; and
4. Data-structure and computer-science utilities (stacks, queues, dynamic arrays, and queued interface mechanisms).

Unlike other simulation programs, MOODS, was not designed to support high-data-volume production runs — although it can be modified to be driven with external input files.

MOODS can be modified easily to support changing analysis requirements. Its kernel set of software tools is exhaustive; this facilitates extensions of the program. If a developmental code is based largely on pre-existing reusable components, then only a minimal amount of new code is needed. Moreover, MOODS requires frequent recompilation of its input unit; this makes initialization of a MOODS simulation extremely flexible.

MOODS must be flexible because it works in a rapidly changing environment; more specifically, in its original application in the U.S. space program, it simulates the trajectories of a large number of orbital objects. The main subsystems of MOODS as configured for this application (see figure) are (1) a simulation executive subsystem, (2) an environment subsystem, (3) a set of reusable utilities, (4) a hardware subsystem, and (5) a flight-software subsystem. The machine-independent MOODS kernel comprises the first three mentioned subsystems.

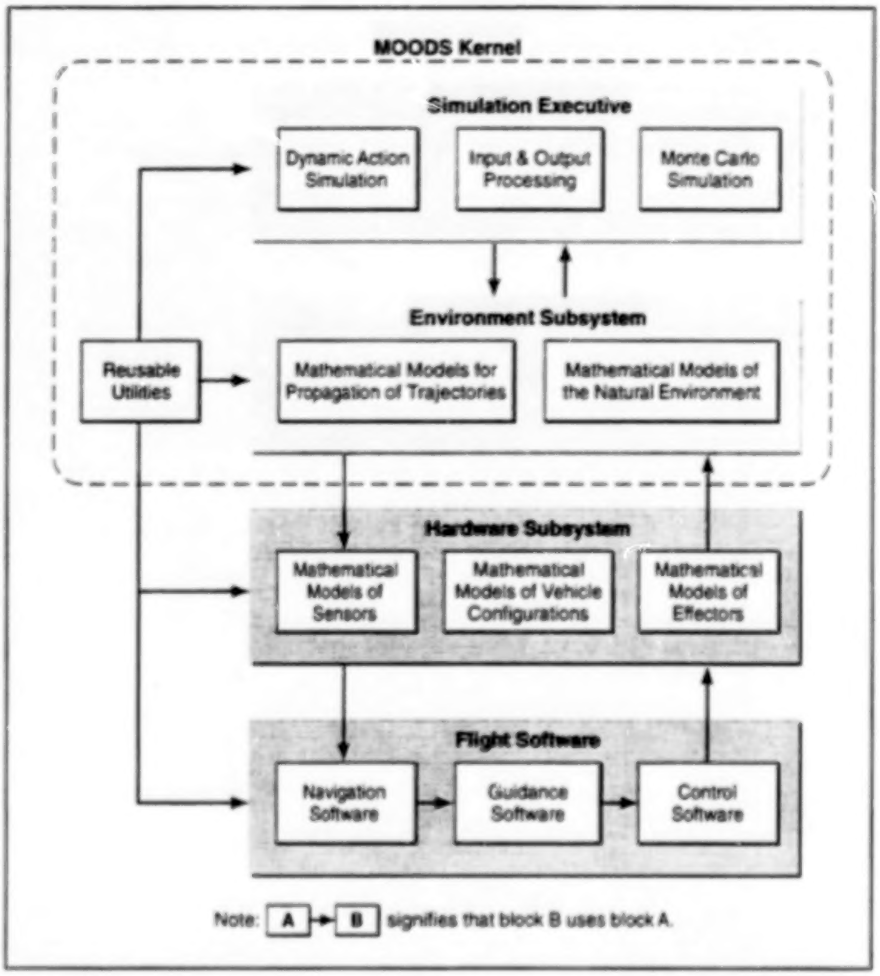

The MOODS Software System is general, extensible, easily modifiable, and reusable. In the configuration depicted here, MOODS is used to simulate trajectories of many orbital objects.

The MOODS kernel is a collection of roughly 211 Ada units. Its source code is partitioned on a VAC computer into 347 files that occupy 1.9MB of memory space. The object code occupies 602KB of memory space. Because each kernel utility is generic and reusable, extension of the capability of the program involves only a minimal amount of development of new code.

The uniqueness and greatest strength of MOODS lie in its suitability for system-analysis and -development projects in which frequent changes in dynamics-simulating computer codes are necessary. MOODS is user-friendly. Its flexibility and reusability should prove as valuable to industry as they have already proved in the U.S. space program.

This work was done by Roger W. Corson, Michael J. Little, and Jeffrey S. Patterson of McDonnell Douglas for **Johnson Space Center**. *Further information is contained in a TSP [see page 1].*
MSC-22527

Knowledge-Based Reasoning Tool for Diagnosing a Complex Flow System

This program is designed as a real-time aid to analyze system health.

John F Kennedy Space Center, Florida

The Propulsion Advisory Tool (PAT) is a knowledge-based computer program that monitors real-time data from more than 300 sensors in the space shuttle Main Propulsion System (MPS). The thermal conditions within the launch pad storage/transfer facility, MPS, and External Tank (ET) must be monitored during the propellant-loading process in order to maintain subcooled cryogenic-liquid conditions and prevent an LO_2 geyser. The PAT knowledge base can provide a quick and accurate assessment of an anomaly by identifying both actual and potential system failures in addition to pertinent data for anomaly resolution.

In the terminology of artificial intelligence, this software is characterized as a knowledge-based reasoning tool. The knowledge base is coded using a natural language interface (plain English) and is developed based on existing requirements documents and knowledge captured from experts working in the propulsion arena. In this way, the expert system works within a framework similar to the way humans would; a system based on human logic and reasoning on quantitative real-time data.

The knowledge base was developed using a hybrid methodology of commercial off-the-shelf (COTS) tools and custom computer code. The COTS tools currently used in the PAT system are Gensym's G2 expert system shell and Oracle. Relational data bases containing real-time, full-rate shuttle data are used to assess the health of the data coming from the vehicle. The PAT uses rule and model-based approaches for the analysis of system health. Rules are used primarily for limit checking, formulating diagnostics, determining state conditions, and user interface tasks. The model base evaluates system configuration and component connectivity.

Pressure, temperature, and flowrates within the propellant loading system can be calculated, and the information can then be extrapolated in order to infer fluid conditions in other locations. Objects representing pressure and temperature sensors contain both the true system redline conditions and engineering estimates of what their values should be for each phase of the propellant load process. For a visual reference, the current value of key pressure/temperature sensors are plotted against the theoretical saturation curve.

Component electrical circuits have been modeled within the G2 knowledge base to reflect the active current path. The electrical circuit shows "live" wires along with active objects that represent the various talkbacks within the circuit. The power of this feature is that the systems engineer can directly relate the data provided by the orbiter with the paper-based drawings that describe the circuit design.

PAT displays include a page that informs the user of the current step in the propellant-loading procedure. Another display shows the loading system schematic. The components within the system are represented as live objects with user-defined attributes. Selecting these objects displays detailed information about that object. In addition, the fluid lines are colorized based upon the phase conditions of the propellant.

The PAT knowledge base will be part the expert-system tools for the next generation of shuttle-launch-processing software, referred to as the Checkout & Launch Control System (CLCS). In addition, the PAT software is used on the day of launch in the Launch Control Center at KSC for each shuttle mission. The PAT knowledge base architecture has been used as a prototype to design and as a basis for building several expert systems, one of which includes command and control for the ground checkout of flight-test hardware.

This work was done by Laurence H. Fineberg, James M. Engle, Anton C. Melichar, James R. Lane, John A. Marinuzzi, Jose Gallardo, Jim Howarth, Janice L. Lessman, and Manuel Beltran of Boeing North American Corp. for **Kennedy Space Center**.

Inquiries concerning rights for the commercial use of this invention should be addressed to the Patent Counsel, Kennedy Space Center; (407) 867-6225. Refer to KSC-11902.

Software for Qualitative Flow-Path Modeling of Systems

This program can be used in simulating behaviors of systems affected by operational events.

Lyndon B. Johnson Space Center, Houston, Texas

A computer program called "the explicit global-modeling tool" implements a dynamic method of operation by which researchers can (1) determine global flow-path changes that occur during computational simulations of the behaviors of engineering systems; (2) analyze both normal and faulty qualitative system behavior; and (3) identify the corresponding local changes, caused by operational events or failures, in mathematical models of such systems. The program is a generic device-modeling tool that effects a software version of human qualitative analysis of device behavior.

Although progress has been made in qualitative modeling and analysis of perturbations in electrical circuits, by use of graph clustering (which is a continuous system-modeling method), the method implemented in the explicit global-modeling tool provides a significant advance over the continuous system-modeling method. In continuous system modeling, conventional numerical analysis is used to compute quantitative values of the behavior of a system and its components in each steady state. Analysis of dynamics involves solving equations for all proposed topologies and comparing these results to derive changed values; this is a very complex process, and in order to be able to effect the process, one must identify the dynamic topologies and appropriate simplifications and statistical assumptions for the system to be analyzed.

In contrast, the explicit global-modeling tool implements a method compatible with local modeling, discrete simulation, and analysis. Far less complex than any computer program developed previously for the same purpose, this program disentangles important global system-power-transmission variables from

local component variables. This program thus supports abstracted general-purpose local mathematical models, and does not require the development of multiple-system, configuration-specific mathematical models for each component as is required in continuous system modeling.

The basis of the design of the explicit global-modeling tool is a data structure and algorithms in which flow-path elements communicate with one or more parent objects. Each parent object represents a subgraph of an overall flow network in a modeled system. During simulations, the elements report information on their local states, and the parent objects report to their elements the statuses of flow-related attributes of the subgraphs — e.g., whether an external flow into a subgraph occurs because of sources external to that subgraph.

The qualitative method of abstraction used in the explicit global-modeling tool supports the use of discrete-event-simulation approaches in analyzing analog systems. The power-transmission abstraction and clustering approach also afford broad applicability to several discrete and analog domains, and to such analysis domains as reliability block-diagram analysis. The program has already been demonstrated to be especially useful in applications of the type for which it was designed; namely, analysis of spacecraft equipment systems. Other, industrial uses are expected to evolve as the program becomes modified in subsequent development efforts.

This work was done by Jane T. Malin of **Johnson Space Center** *and Land D. Fleming of Hernandez Engineering, Inc. Further information is contained in a TSP [see page 1].*

This invention has been patented by NASA (U.S. Patent No. 5,732,192). Inquiries concerning nonexclusive or exclusive license for its commercial development should be addressed to the Patent Counsel, Johnson Space Center, (281) 483-0837. Refer to MSC-22618.

National Aeronautics and
Space Administration

52

END

03\24\99